

Article

Multi-Objective Optimization-Based Approach for Optimal Allocation of Distributed Generation Considering Techno-Economic and Environmental Indices

Muhammad Shahroz Sultan ¹, Syed Ali Abbas Kazmi ¹, Abdullah Altamimi ^{2,3,*}, Zafar A. Khan ^{4,5,*}
and Dong Ryeol Shin ⁶

- ¹ US-Pakistan Center for Advanced Studies in Energy (USPCAS-E), National University of Sciences and Technology (NUST), H-12, Islamabad 44000, Pakistan
- ² Department of Electrical Engineering, College of Engineering, Majmaah University, Al-Majmaah 11952, Saudi Arabia
- ³ Engineering and Applied Science Research Center, Majmaah University, Al-Majmaah 11952, Saudi Arabia
- ⁴ Department of Electrical Engineering, Mirpur University of Science and Technology, Mirpur AK 10250, Pakistan
- ⁵ School of Computing and Engineering, Institute for Innovation in Sustainable Engineering, University of Derby, Derby DE22 1GB, UK
- ⁶ Department of Electrical and Computer Engineering, College of Information and Communication Engineering (CICE), Sungkyunkwan University (SKKU), Suwon 16419, Republic of Korea
- * Correspondence: a.altamimi@mu.edu.sa (A.A.); zafarakhan@ieee.org (Z.A.K.)

Abstract: Distribution networks have entered a new era with the broad adoption of the distributed generation (DG) allocation as a practical solution for addressing power losses, voltage variation, and voltage stability. The primary goal is to enhance techno-economic and environmental characteristics while meeting the limitations of the system. In order to allocate DGs in active distribution networks (ADNs) efficiently, this study demonstrates two optimization methods inspired by nature: ant lion optimization (ALO) and multiverse optimization (MVO). Various multi-criteria decision-making (MCDM) methods are used to find the best possible solution among the different alternatives. On the IEEE 33- and 69-bus active distribution networks, the proposed ALO was shown to be effective and produces the highest loss reduction in the IEEE 33- and 69-bus systems at 94.43% and 97.16%, respectively, and the maximum voltage stability index (VSI) was 0.9805 p.u and 0.9937 p.u, respectively; moreover, the minimum voltage deviation (V_D) and annual energy loss cost for the given test systems was 0.00019 p.u and 3353.3 PKR, which shows that the suggested method can produce higher quality results as compared to other methods presented in the literature. Therefore, the proposed ALO is a very efficient, effective, and appealing solution to the optimal allocation of the distributed generation (OADG) problem.

Keywords: ant lion optimization; distributed generation; greenhouse gas (GHG) emissions; multi-objective optimization; optimal allocation; optimal size



Citation: Sultan, M.S.; Kazmi, S.A.A.; Altamimi, A.; Khan, Z.A.; Shin, D.R. Multi-Objective Optimization-Based Approach for Optimal Allocation of Distributed Generation Considering Techno-Economic and Environmental Indices. *Sustainability* **2023**, *15*, 4306. <https://doi.org/10.3390/su15054306>

Academic Editor: Nicu Bizon

Received: 2 November 2022

Revised: 21 November 2022

Accepted: 25 November 2022

Published: 28 February 2023



Copyright: © 2023 by the authors. Licensee MDPI, Basel, Switzerland. This article is an open access article distributed under the terms and conditions of the Creative Commons Attribution (CC BY) license (<https://creativecommons.org/licenses/by/4.0/>).

1. Introduction

The distribution system causes a significant voltage drop and a low voltage stability due to its high R/X ratio [1]. Energy resources are a global concern and energy consumption measures are society's development. Industrial, economic, and social changes are boosting load demand. The challenge is providing enough power efficiently and affordably. Microgrids and multi-microgrids have been gaining traction all over the world due to the increasing use of distributed energy resources (DERs) in the last decade. The modern grid has several advantages over the traditional grid, but some shortcomings, such as power losses, power quality, and voltage instability, need to be addressed to make the system

reliable. The advantages of allocating DGs at the optimal locations into the distribution system entail technical, economic, and environmental benefits. Power loss minimization, voltage profile improvement, and system stability enhancement are considered technical benefits of the optimal allocation of DGs (OADG). Economically, it helps in reducing power loss costs and increases annual loss savings. Placing the renewable generations of optimal sizes at optimal locations helps to reduce environmental effects, such as greenhouse gas (GHG) emissions.

DG units are either classified as conventional (diesel engines) or renewable (solar and wind power). Their penetration has changed the structure of the radial distribution system (RDS) from passive to active and the unidirectional flow of power to multi-directional [2]. In order to obtain the above-mentioned benefits from the integration of DGs, and to avoid its negative impacts, such as reverse power flow, high power losses, and unfavorable voltage levels [3], the optimal sizing and siting of DGs are of significant importance. The OADG has been an exciting and challenging problem to focus on. Therefore, researchers have taken various studies and developed different optimization techniques to address this problem.

This research article proposed two efficient, nature-inspired metaheuristic optimization techniques, known as ant lion optimization (ALO) [4] and multiverse optimization (MVO) [5], to solve the optimal sizing and siting problems of distributed generation. The ALO has been used in different optimization problems, such as the scheduling of generation, flexible process planning, and structure design of the skeletal structure [6–8], respectively. Similarly, the MVO has also shown its effectiveness in solving various optimization problems. Moreover, in this paper, the OADG problem is solved as a multi-objective optimization problem considering techno-economic and environmental attributes. The objectives include active and reactive power loss reduction, voltage deviation (V^D) minimization, voltage stability index (VSI) enhancement, annual energy loss cost (C_{AEL}) reduction, and annual energy loss cost saving (S_{AEL}) subjected to voltage and power constraints. Figure 1 shows the framework of the proposed work. The main contribution of this research paper can be summarized as follows.

- (i) An efficient optimization approach is used to identify the appropriate allocation of DG units in the active distribution system.
- (ii) The main objectives are to minimize the total power losses and voltage deviation and to maximize the VSI, thus lowering the yearly energy loss costs and carbon emissions.
- (iii) IEEE 33- and 69-bus ADNs are used to test the effectiveness of the proposed technique.
- (iv) The suggested ALO's efficacy is compared to MVO and other well-known optimization approaches at various operating scenarios.
- (v) The functioning of DG units at various power factors is investigated. It was observed that when DGs run at optimal power factors, the total performance of an ADN (techno-economic and environmental benefits) is greatly increased.
- (vi) Several MCDM methodologies are employed to find the best trade-off among the available alternatives.

The following is how this paper is structured: Section 2 highlights the relevant work conducted by the researchers in recent years. Section 3 discusses the methodology, covering the primary objective functions and MCDM approaches in-depth, as well as an overview of the algorithms utilized. The numerical findings based on the test systems are reported in Section 4. Finally, in Section 5, the conclusion is discussed.

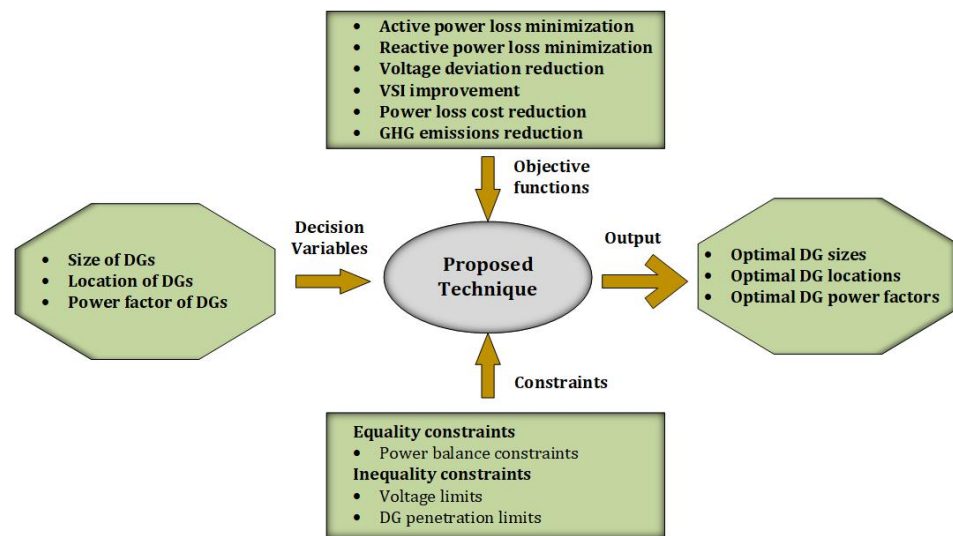


Figure 1. Development of proposed technique (adapted from [9]).

2. Literature Review

The algorithms for solving OADG problems can be classified into different categories, such as analytical [10–12], numerical [13–15], and intelligent search-based methods [16–18]. The problem of the optimal sizing and siting of DGs has been solved by many researchers, either by considering a single-objective optimization problem (SOOP) or a multi-objective optimization problem (MOOP). Power loss reduction has been the primary objective in the SOOP, whereas for the multi-objective one, power loss minimization, voltage stability enhancement, voltage deviation reduction, and cost minimization are considered simultaneously.

In [19], the authors hybridized analytical and heuristic strategies to solve the OADG and minimize power losses. The size of the DGs was computed analytically, and particle swarm optimization (PSO) was used to find their optimal locations. The suggested method was tested on IEEE 33- and 69-bus systems. The authors of [20] determined the optimal location of DGs to reduce power losses by using analytical methods while considering both radial and meshed distribution systems. The OADG problem in [15] was solved using mixed-integer linear programming and the steady-state behavior of the RDS was modeled using linear expressions at different load levels. Mixed-integer linear programming (MILP) was used in [21] to reduce power losses in the radial distribution network (RDN). The authors used single- and multi-objective improved Harris hawk optimization algorithms (IHHO) to tackle the OADG problems at varied power factors [2]. The fundamental objective of the incorporation of DG was to enhance voltage profiles and lower power losses, which will ultimately lead to a rise in the overall efficiency of the power system [22].

The OADG technical, economic, and environmental concerns were solved using a stochastic multi-objective model [23]. A modified version of grey wolf optimization (GWO) was used in [24] to optimally place DGs, considered techno-economic benefits. Various loads (commercial, industrial, residential, constant power, current, and impedance) were considered at different loading levels, such as a full, light, and heavy load. A multi-objective function was presented in [25] for the optimal placement of DGs to minimize losses and improve reliability; a time-varying load was used to achieve the practical outcomes, while the entire study and its requirements were based on a cost–benefit analysis. The authors of [26] addressed power loss reduction, high voltage stability, and voltage profile enhancement by combining PSO and GA while considering operational and security constraints. The IEEE 33- and 69-bus systems were utilized to highlight the usefulness of the suggested method. A new hybrid solution based on an evolutionary algorithm and intelligent water drop (IWD) algorithm improved the voltage stability, reduced the voltage deviation, and minimized the power loss for the IEEE 33- and 69-bus systems [27]. The author presented a novel method for determining the DG placement and size to reduce

losses, operating costs, and voltage instability. The loss sensitivity factor (LSF) was used to discover the most sensitive bus for a DG installation [28].

Ant colony optimization (ACO) and the artificial bee colony (ABC) were hybridized to resolve the location and sizing problem of DGs in distribution networks. The cost, loss, and GHG emission reductions were discussed [29]. Similarly, the optimal DG placement and sizing problems were discussed in [30–33] by using various optimization algorithms. GA was employed for siting while the optimal power flow was used for the DG sizing. The proposed methodology was tested in the UK under the existing gem financial incentives for DNOs and was effective in finding and sizing DG units [30]. In [31], evolutionary programming was utilized to optimally arrange PV arrays and wind turbine generators (WTG). Probabilistic techniques were used to deal with the load and renewable resource uncertainty, and a 69-bus distribution test system was used to test the devised approach. The authors of [32] addressed multiple objectives to give economical solutions to solve the OADG problem by using GA and the ϵ -constrained method. To provide power system stability, protection devices and distributed generators (DGs) in radial feeders must be optimized. The authors proposed a technique to properly arrange DGs and protection devices in an RDS to improve the system reliability [33].

The optimal allocation of wind and solar in terms of the objective function while accounting for uncertainties was found using lightning attachment procedure optimization (LAPO) in an RDN; the effectiveness of the proposed method was verified using a 118-bus system, and the results validated the efficacy of the proposed algorithm [34]. In a cost–benefit analysis, the elephant herding optimization (EHO) algorithm was applied and evaluated on IEEE 15-bus, 33-bus, and 69-bus systems. The proposed algorithm with a type-III DG unit operating at 0.9 pf produces better results [35]. To decrease the active power loss and boost the voltage stability index while solving the OADG problem, a multi-objective BAT algorithm (BA) was employed in [36]. The manta ray foraging optimization technique, also known as MRFO, was applied in [37] to figure out the location and capacity of type-one DGs for the purpose of cutting down on power losses in an RDN. The authors of [38] used an improved raven roosting optimization (IRRO) method to boost the techno-economic advantages of DG deployment in the radial distribution system (RDS), and the IEEE 33- and 69-bus systems were the test systems to check the effectiveness of the proposed technique. In [39], the power losses were minimized under deterministic factors and the validity was tested on IEEE 69- and 118-bus systems.

Researchers around the world have attempted to deal with the asset planning's multiple distribution strategy restrictions. The methodologies identify a trade-off between numerous competing objectives. These trade-off solutions could be techno-economic or environmental, or both [40]. Several works based on MCDMs on the axis of grid-connected ADNs, such as [41,42], have sought to fulfill the largely technical and economic objectives while incorporating radiality constraints and spanning normal load situations without evaluating large-scale planning horizons. The technical, economical, and environmental-based strategy is used simultaneously in [43] across typical loading scenarios at different power factors associated with REGs in radially constructed ADNs.

According to this literature review, most of these population-based optimization strategies have been effectively applied to estimate the size, location, and loss reduction problem of DG in the active distribution system. However, many of them suffer from local optimality and need a significant amount of computational power to simulate. This motivates the authors to provide a new, simple, efficient, and rapid population-based optimization approach for solving the optimum DG placement problem of the radial distribution system. Another significant observation is that, for the multi-objective problem, most of the studies only look at DGs with the unity power factor, and only a few studies explore the applicability of the proposed method to large-scale networks, whereas in this paper, many operating modes (the unity, fixed, and optimal power factors) for DGs are considered. Many researchers have presented their work focusing on one of the components of the objective functions (technical, economic, and environmental), while in this study,

simultaneously the techno-economic and environmental attributes are taken into account while solving the OADG problem.

3. Methodology

This section highlights the objective functions that are considered for addressing the optimum allocation of DG problem, as well as the details of the methodologies used.

3.1. Objective Functions

The issue of DG allocation requires special attention to the formulation of the objective function and specific limitations must be properly modeled. The primary goal of the optimal allocation of DGs in the distribution system is to attain desired objectives by satisfying equality and inequality constraints. The proposed objective functions are power loss reduction, maximization of voltage stability index, voltage deviation minimization, real power loss cost reduction, increasing real power loss savings, and CO₂ emissions reduction. Figure 2 shows a branch of an active distribution network having P_b and Q_b as active and reactive power at receiving end, respectively.

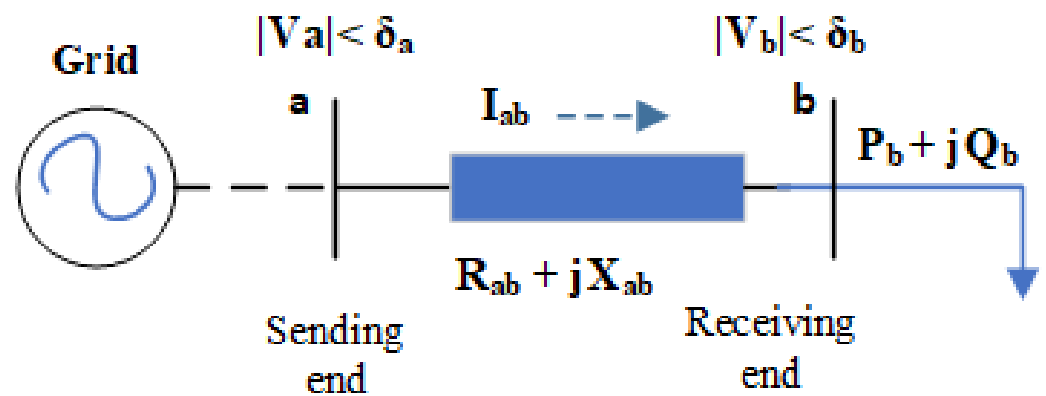


Figure 2. A representative branch of RDS (adapted from [44]).

3.1.1. Active Power Loss (P_L)

As active power losses in distribution networks are significant due to their radial topology, it is necessary to mitigate these losses to make the system stable and reliable.

$$OF_1 = \min(P_L) \quad (1)$$

Mathematically, (P_L) is expressed in [44] as

$$P_L = \frac{R_{ab}}{V_a V_b} \left(\sum_{a=1}^n \sum_{b=1}^n \cos(\delta_a - \delta_b) * (P_a P_b + Q_a Q_b) + \sin(\delta_a - \delta_b) * (Q_a P_b - Q_b P_a) \right) \quad (2)$$

a and b are two different buses in which power loss is being calculated. V_a , δ_a are voltage magnitude and angle at bus a, respectively, similarly V_b , δ_b are voltage magnitude and angle at bus b, respectively. P_a and Q_a are real and reactive power at bus a; similarly, P_b and Q_b show real and reactive power at bus b. P_L is calculated in [9] by following relation.

$$P_L = \sum_{b=1}^N |I_b|^2 R_b \quad (3)$$

b is the number of the branch, whereas $|I_b|$ and R_b show the absolute value of the current and resistance of the branch, respectively. Another dimension of the above-mentioned objective is to maximize the percentage reduction in power loss, which may be determined

using (4) in which $P_{L_{bc}}$ shows base-case (without DG) power loss and $P_{L_{wdg}}$ represents power loss with DGs.

$$\%P_L = \left[\frac{P_{L_{bc}} - P_{L_{wdg}}}{P_{L_{bc}}} \right] \times 100 \quad (4)$$

3.1.2. Reactive Power Loss (Q_L)

Minimization of reactive power losses (Q_L) is of great importance in OADG problem.

$$OF_2 = \min(Q_L) \quad (5)$$

In [45], reactive power loss is calculated by

$$Q_L = \sum_{b=1}^N |I_b|^2 X_b \quad (6)$$

In (6), b is the number of branches, whereas $|I_b|$ and X_b show the absolute value of the current and reactance of the branch, respectively.

3.1.3. Voltage Stability Index (VSI)

VSI is the ability of the system to maintain the voltage within the satisfactory range. The primary goal is to maximize the lowest VSI in the system [46].

$$OF_3 = \max(\text{lowest}(VSI_b)) \quad (7)$$

$$VSI_b = V_a^4 - 4(P_b R_{ab} + Q_b X_{ab}) * V_a^2 - 4(P_b X_{ab} - Q_b R_{ab}) \quad (8)$$

In (8), a is sending-end bus and b is receiving-end bus, P_b and Q_b are active and reactive power of receiving-end bus, respectively, whereas R_{ab} and X_{ab} show resistance and reactance between two buses, respectively.

3.1.4. Voltage Deviation (V_D)

$$OF_4 = \min(V_D) \quad (9)$$

Voltage deviation shows the deviation of voltage from its reference voltage (V_{ref}) which is 1.0 p.u.

$$V_D = \sum_{a=1}^n (V_a - V_{ref})^2 \quad (10)$$

3.1.5. Annual Energy Loss Cost (C_{AEL})

C_{AEL} demonstrates the validity of the proposed technique from a cost perspective. The aim of this objective is to lower the annual cost of energy loss.

$$OF_5 = \min(C_{AEL}) \quad (11)$$

Equation (12) is used to calculate energy loss cost [47].

$$C_{AEL} = P_L * \mu_E * t \quad (12)$$

where

P_L is the power loss;

μ_E is the rate of energy (PKR/kWh);

t is the time (8760 h).

As we are dealing with annual energy cost, “ t ” is 8760 h and μ_E is taken as 0.06 PKR/kWh.

3.1.6. Annual Energy Loss Cost Saving (S_{AEL})

S_{AEL} can be calculated by (13)

$$S_{AEL} = C_{AEL-bc} - C_{AEL-dg} \quad (13)$$

3.1.7. Greenhouse Gas Emissions (GHG_E)

While considering environmental effects, several studies in the literature seek to identify the determinants of carbon dioxide (CO_2) emissions because of large increases in CO_2 emissions over the last few decades. So, the solution to the problem must meet environmental demands, and the above-mentioned objective is to determine whether the solution provided is environmentally feasible or not. Carbon emissions (C_E) are calculated in [48] by (14) and (15)

$$C_{E_{bc}} = \sum_{a=1}^x (G_E)_a * (\mu_e)_a \quad (14)$$

$$C_{E_{wdg}} = \sum_{a=1}^x (G_E)_a * (\mu_e)_a + \sum_{b=1}^y (DG_E)_b * (\mu_e)_b \quad (15)$$

$C_{E_{bc}}$ and $C_{E_{wdg}}$ show CO_2 emissions in the base case (without DG) and with DG, respectively. G_E , DG_E represent energy generated by grid and DG, respectively, whereas μ_e shows CO_2 emissions rate, and it is different for different sources [49].

3.2. Operational Constraints

The issue of DG allotment in the distribution framework ought to be exposed to two following constraints.

1. Equality constraints.
2. Inequality constraints.

3.2.1. Equality Constraints

Power Balance Constraints

The principle of equilibrium upholds equality constraints. The power flow equations that correspond to both the real and reactive power balance equations are mathematically defined as follows [29]

$$P_a = V_a \sum_{b=1}^n V_b Y_{ab} \cos(\theta_{ab} - \delta_a + \delta_b) \quad (16)$$

$$Q_a = V_a \sum_{b=1}^n V_b Y_{ab} \sin(\theta_{ab} - \delta_a + \delta_b) \quad (17)$$

where P_a and Q_a are real and reactive power at bus a, V_a and δ_a are voltage magnitude and its angle at a^{th} bus, respectively. The magnitude and angle of admittance between bus a and b are shown by Y_{ab} and θ_{ab} , respectively. Power flow should follow the following equations to fulfill the equality constraint's requirements.

$$P_{Gen} = P_{load} + P_{loss} \quad (18)$$

$$Q_{Gen} = Q_{load} + Q_{loss} \quad (19)$$

3.2.2. Inequality Constraints

Voltage Limits

The total voltage generated is divided into two parts; some of the voltage appears across the load and some part of it is dropped across the line/impedance. The higher the impedance, the higher the voltage drop, but the voltage limit constraint states that the

voltage across the bus must be within the acceptable range. This paper considers that range to be 0.90 to 1.05.

$$V_{a_MIN} \leq V_a \leq V_{a_MAX} \quad (20)$$

a shows the bus number.

a = 1, 2, 3 ... N

DG Capacity Limits

The size of DGs must be within their minimum and maximum allowable limits.

$$P_{a_MIN}^{DG} \leq P_a^{DG} \leq P_{a_MAX}^{DG} \quad (21)$$

In (21), $P_{a_MIN}^{DG}$ and $P_{a_MAX}^{DG}$ show the minimum and maximum range of power output at bus a, whereas P_a^{DG} shows power output at a^{th} bus.

3.3. Multi Criteria Decision Making (MCDM)

To solve decision-making problems that include a set of predetermined solutions, multi-criteria decision-making (MCDM) techniques are applied. To assess energy planning based on technical, economical, and environmental aspects, MCDM methods are utilized. The evaluation procedure has become more complex and time-consuming as additional criteria and options have been added. If it comes to incorporating significant or delicate criteria, different strategies take different approaches, but when multiple situations, circumstances, and limits are taken into account, MCDM models are best suited to come up with a good answer. This paper discusses several MCDM models, such as WSM, WPM, TOPSIS, and VIKER, that can be used to address the key issues that must be addressed in order to accomplish sustainability objectives.

3.3.1. Weighted Sum Method (WSM)

WSM is one of the most widely used strategies for computing rank, with the goal of finding the best answer among numerous options in terms of the highest score. Equation (22) chooses the solution with the highest score as the best among m alternatives based on n criteria.

$$S_j^{WSM} = \sum_{k=1}^m N_k^j W_k \quad (22)$$

where S_j^{WSM} indicates the weighted sum score, N_k^j is the normalized score of jth alternative/solution from the reference of kth criterion, and W_k is the weight associated with the kth criterion. To rank the best, use the significant cardinal scores for each choice. The option with the highest score is regarded as the best option.

3.3.2. Weighted Product Method (WPM)

The weighted product method is an MCDM method that is used to choose the best alternative based on numerous criteria, and the optimal solution is found by using multiplication rather than addition, with the goal of determining ranks of alternatives as illustrated in WSM. In a pairwise comparison, the best answer is the one with the highest score, as indicated in the equation below.

$$P_j^{WPM} = \prod_{k=1}^m (N_k^j)^{W_k} \quad (23)$$

where P_j^{WPM} indicates the weighted product score.

3.3.3. Technique for Order of Preference by Similarity to Ideal Solution (TOPSIS)

This method is based on the idea of calculating the distance between two hypothetical solutions: the negative ideal solution (NIS) and the positive ideal solution (PIS). The ideal

option should be the one with the least geometric distance from the best solution and the greatest geometric distance from the worst. This method can be summarized in the following steps:

The normalized decision matrix can be calculated as:

$$N_k^j = \frac{S_{jk}}{\sqrt{\sum_{j=1}^n S_{jk}^2}} \quad (24)$$

The weighted normalized decision matrix X_{jk} is calculated as:

$$Y_{jk} = N_k^j * W_k \quad (25)$$

Determine the best (PIS) and the worst (NIS) alternative by Equations (26) and (27), respectively.

$$Y_k^b = \left\{ \left(\max_{j=1}^n Y_{jk} | k \in K \right), \left(\min_{j=1}^n Y_{jk} | k \in K' \right) \right\} \quad (26)$$

$$Y_k^w = \left\{ \left(\min_{j=1}^n Y_{jk} | k \in K \right), \left(\max_{j=1}^n Y_{jk} | k \in K' \right) \right\} \quad (27)$$

where K is the set of beneficial criteria and K' is a set of non-beneficial criteria, and the Euclidean distance from each alternative can be calculated as:

$$E_j^b = \left(\sum_{k=1}^m (Y_{jk} - Y_k^b)^2 \right)^{1/2}, j = 1, 2, 3, \dots, n \quad (28)$$

$$E_j^w = \left(\sum_{k=1}^m (Y_{jk} - Y_k^w)^2 \right)^{1/2}, j = 1, 2, 3, \dots, n \quad (29)$$

For measuring the proximity of the available alternatives, the relative similarity of each option to and from the ideal solutions is determined.

$$P_j = \frac{E_j^w}{E_j^b + E_j^w}, 0 \leq P_j \leq 1, j = 1, 2, 3, \dots, n \quad (30)$$

The best solution can be determined by (30).

3.3.4. VIKOR

The procedure of ViseKriterijumska Optimizacija I Kompromisno Resenje (VIKOR) is indicated as follows.

For all beneficial and non-beneficial criterion functions, determine the best and worst values.

$$S_k^b = \left\{ \left(\max_{j=1}^n S_{jk} | k \in K \right), \left(\min_{j=1}^n S_{jk} | k \in K' \right) \right\} \quad (31)$$

$$S_k^w = \left\{ \left(\min_{j=1}^n S_{jk} | k \in K \right), \left(\max_{j=1}^n S_{jk} | k \in K' \right) \right\} \quad (32)$$

where

$K \in$ is set of beneficial criteria;

$K' \in$ is set of non-beneficial criteria.

The normalized decision matrix N_k^j is calculated as:

$$N_{jk} = (S_k^b - S_{jk}) / (S_k^b - S_k^w) \quad (33)$$

Compute utility measure S_j and regret measure R_j by using the following equations.

$$S_j = \sum_{k=1}^m (W_k * N_{jk}) \quad (34)$$

$$R_j = \max_{k=1}^m (W_k * N_{jk}) \quad (35)$$

Now, calculate the VIKOR index by the equation given below

$$Q_j = v \left[\frac{S_j - S^*}{S^- - S^*} \right] + (1 - v) \left[\frac{R_j - R^*}{R^- - R^*} \right] \quad (36)$$

where

$$S^* = \min_j S_j;$$

$$S^- = \max_j S_j;$$

$$R^* = \min_j R_j;$$

$$R^- = \max_j R_j.$$

The weight for the greatest group utility strategy is v , which is commonly set to 0.5 for a balanced approach. The best accessible solution is determined as the alternative with the lowest VIKOR value.

3.4. Overview of Optimization Techniques

The following optimization techniques are used in this paper to solve the OADG problem:

1. Ant lion optimization (ALO).
2. Multiverse optimization (MVO).

3.4.1. Ant Lion Optimization

ALO is an efficient, nature-inspired, metaheuristic optimization Algorithm 1 presented by Mir Jalili [4] in 2015. ALO imitates the natural hunting mechanism of ant lions, and it can be used to solve different optimization problems because of its balancing capability between exploration and exploitation. This method consists of a random walk exploration followed by a random selection of agents, and the exploitation process is performed with traps. By moving in a circular pattern and pushing sand out with its jaws, an ant lion larva creates a cone-shaped trench in the sand [50]. The larva hides beneath the bottom of the cone after digging the trap and waits for insects to be captured in the pit [51]. The pointed edge of the cone allows insects to readily fall to the bottom of the trap. When the ant lion discovers a prey in the trap, it strives to capture it. Then, it is sucked into the ground and eaten. Ant lions prepare the pit again after eating the prey and tossing the remains outside of the pit [52]. ALO follows five basic steps of ant lions for hunting.

1. Random walk of agents.
2. Trap building.
3. Trapping of ants.
4. Capturing prey.
5. Trap reconstruction.

The explanation of each step with its mathematical modeling is as follows.

Random Walk of Agents

While searching for prey, ants often move in a stochastic manner, and this randomness can be modeled by (37)

$$X(t) = [0, \text{csum}(2r(t_1) - 1), \text{csum}(2r(t_2) - 1) \dots \text{csum}(2r(t_n) - 1)] \quad (37)$$

where *csum* means cumulative sum and $r(t)$ can be defined as

$$r(t) = \begin{cases} 0 & \text{if rand} \leq 0.5 \\ 1 & \text{if rand} > 0.5 \end{cases} \quad (38)$$

In (38), *rand* will generate a random number between 0 and 1. If this random number is less than or equal to 0.5, then it will assign value 0 to $r(t)$; otherwise, value 1 will be assigned to $r(t)$. Equation (37) shows that ants changed their position randomly, so to normalize their position and to fulfill boundary constraints, following equation can be used.

$$X_i^t = \frac{[(X_i^t - V_i) \times (Z_i^t - Y_i^t)]}{W_i - V_i} + Y_i^t \quad (39)$$

Equation (39) is used to make sure that random walk must be in search space, so it can be used in every iteration. Minimum and maximum walk of i^{th} variable is shown by V_i and W_i , respectively, whereas Y_i^t and Z_i^t show lower and upper extreme values of i^{th} variable at t^{th} iteration.

Trap Building

A roulette wheel operator is used to simulate the hunting activity of ant lions. During the optimization phase, this operator is used to choose the ant lions based on their fitness value. This strategy increases the chances of the ant lions catching the prey.

Algorithm 1: Pseudo Code of ALO

```

Initializing ALO parameters
Set initial values
Initialize ants and antlions positions
for  $i = 1 : 50$  do
  | calculate initial fitness values for ants and antlions
end
sort best fitness value and set it as elite
while  $current\_iter < max\_iter + 1$  do
  | for each ant do
  |   | find antlion using roulette wheel
  |   | update values of  $y$  and  $z$  by (42) and (43)
  |   | simulate and normalize a random walk by using (37) and (39)
  |   | update ant position
  | end
  | Bring antlions back if they go beyond boundaries
  | calculate fitness
  | replace antlion with corresponding fitter ant by using (44)
  | update the position of the elite if any antlion becomes fitter than it.
end

```

Trapping of Ants

Ant lions' traps affect the random movements of ants in a search space. The following equations mathematically illustrate the effect of ant lions' traps on the random movement of ants.

$$Y_i^t = AntL_j^t + Y^t \quad (40)$$

$$Z_i^t = AntL_j^t + Z^t \quad (41)$$

Y^t and Z^t are vectors that show the values of variables at t^{th} iteration, and $AntL_j^t$ refers to position of j^{th} ant lion at t^{th} iteration.

Sliding Ants toward Ant Lions

Using the above-mentioned processes, the ant lions build the traps according to their fitness value. Ant lions start throwing the sand outward from the center of the trap, once randomly moving ants get trapped near the traps, and this eliminates the possibility of ants escaping. The radius of random ant walks in the hypersphere is adaptively decreased. Equations (42) and (43) can be used to mathematically reflect this process.

$$y^t = \frac{y^t}{I} \quad (42)$$

$$z^t = \frac{z^t}{I} \quad (43)$$

y^t and z^t are vectors that show max and min values of variables at t^{th} iteration and $I = 10^W t/T$ where t denotes the current iteration, T shows a total number of iterations, and W depends upon the current iteration.

Capturing Prey and Trap Building

In this step, the focus is catching prey by ant lions (predators) and rebuilding traps for catching new prey (ants). To depict this mechanism, it is assumed that prey can only be grabbed when ants become fitter than ant lions. The mathematical form of this step is shown below.

$$\text{AntL}_j^t = \text{Ant}_i^t \quad \text{if } f(\text{Ant}_i^t) > f(\text{AntL}_j^t) \quad (44)$$

Variables in (44) show position of i^{th} ant and j^{th} ant lion at t^{th} iteration.

Elitism

The best ant lion solution is regarded as elite in each iteration of the ALO algorithm. As the elite is the finest ant lion, it should be able to dominate the whole movements of the other ants throughout the iterations. The following mathematical equation is used to illustrate the elitism process.

$$\text{Ant}_i^t = \frac{(R_a^t + R_e^t)}{2} \quad (45)$$

In Equation (45), R_a^t and R_e^t show random walk of ants around ant lions and elite, respectively. Pseudo code for ALO is given and Figure 3 shows the flow chart for proposed ant lion optimization.

3.4.2. Multiverse optimization

A proposed multiverse optimizer is a unique stochastic population-based Algorithm 2 presented in 2015 [5]. MVO is based on the multiverse theory of physics and MVO can be presented mathematically by using three major ideas from this theory:

1. White hole.
2. Black hole.
3. Worm hole.

The multiverse theory states that objects are traded between worlds via black, white, and wormholes. Things are sent through white holes in universes having greater inflation rates, whereas universes with low inflation rates are used to receive objects through black holes. The following is the mathematical model for white and black hole tunnels and item transfer across universes.

$$V_i = [y_i^1 \quad y_i^2 \quad y_i^3 \quad \dots \quad y_i^n] \quad (46)$$

V_i in (46) shows i^{th} universe, total number of decision variables are represented by n , and y_i shows i^{th} candidate's decision variable. To locate the universe containing the white hole, utilize the roulette wheel approach as follows.

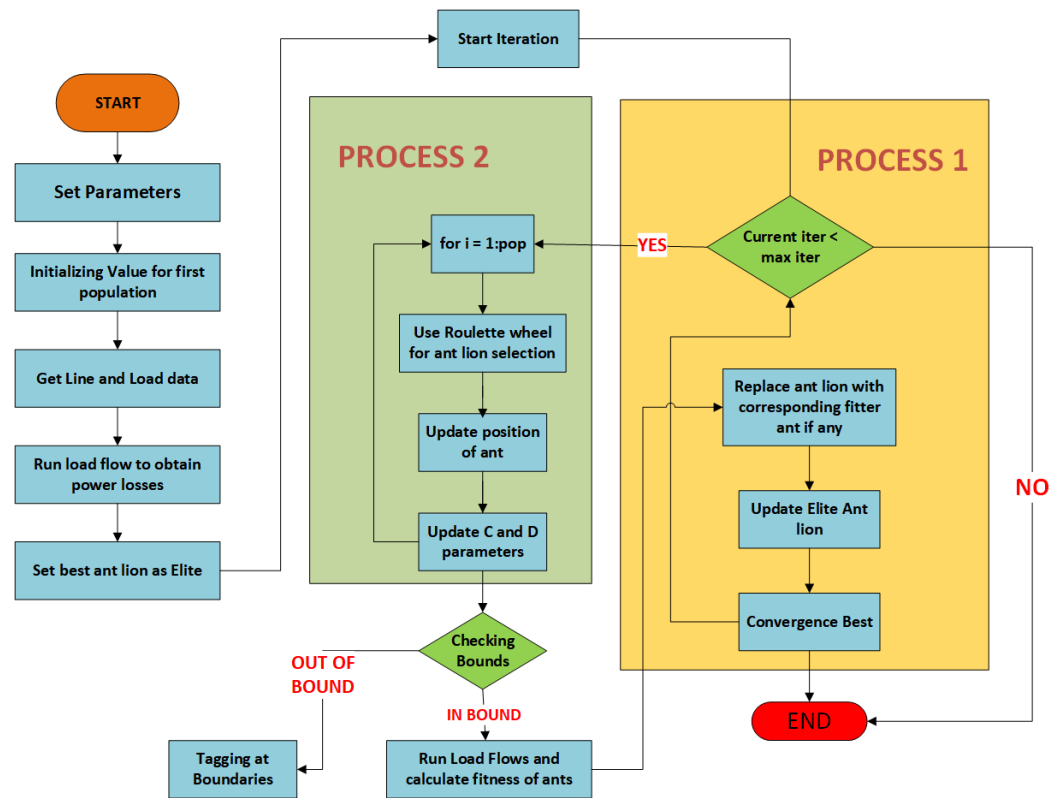


Figure 3. Flow chart of proposed ALO.

$$y_i^j = \begin{cases} y_s^j & \text{rand} < \text{norinf}(V_i) \\ y_i^j & \text{rand} \geq \text{norinf}(V_i) \end{cases} \quad (47)$$

rand in (47) shows random number between [0,1] and *norinf* shows normal inflation rate, whereas y_s^j shows j^{th} variable of s^{th} universe. The above equation shows that universes with higher inflation rates are more likely to have a white hole, whereas universes with lower inflation rates are more likely to contain a black hole. By this strategy, we can improve the exploration phase, whereas for the improvement in exploitation phase, objects are exchanged among universes through worm holes. The mathematical expression for this step is shown in (48). $rand_2$ and $rand_3$ show a random number between 0 and 1, whereas the lower bound and upper bound are denoted in (48) by lb and ub , respectively. Values of TDR and WEP can be calculated by using (49) and (50), respectively.

$$y_i^j = \begin{cases} \begin{cases} y_c^j + TDR[(ub_i - lb_i) \text{rand} + lb_i] \\ \text{rand}_1 < 0.5 \end{cases} & \text{if } \text{rand}_2 < \text{WEP} \\ \begin{cases} y_c^j + TDR[(ub_i - lb_i) \text{rand} + lb_i] \\ \text{rand}_1 \geq 0.5 \end{cases} & \text{if } \text{rand}_2 \geq \text{WEP} \\ y_i^j & \end{cases} \quad (48)$$

$$TDR = 1 - \left(\frac{\text{iter}^{\frac{1}{p}}}{\text{iter_max}} \right) \quad (49)$$

$$WEP = WEP_{MIN} + \frac{\text{iter}(WEP_{MAX} - WEP_{MIN})}{\text{iter_max}} \quad (50)$$

iter_max is the maximum number of iterations and iter is the current iteration, whereas

WEP_{MAX} , WEP_{MIN} , and P are constants. Pseudo code of MVO is given, and Figure 4 shows a flow chart of multiverse optimization.

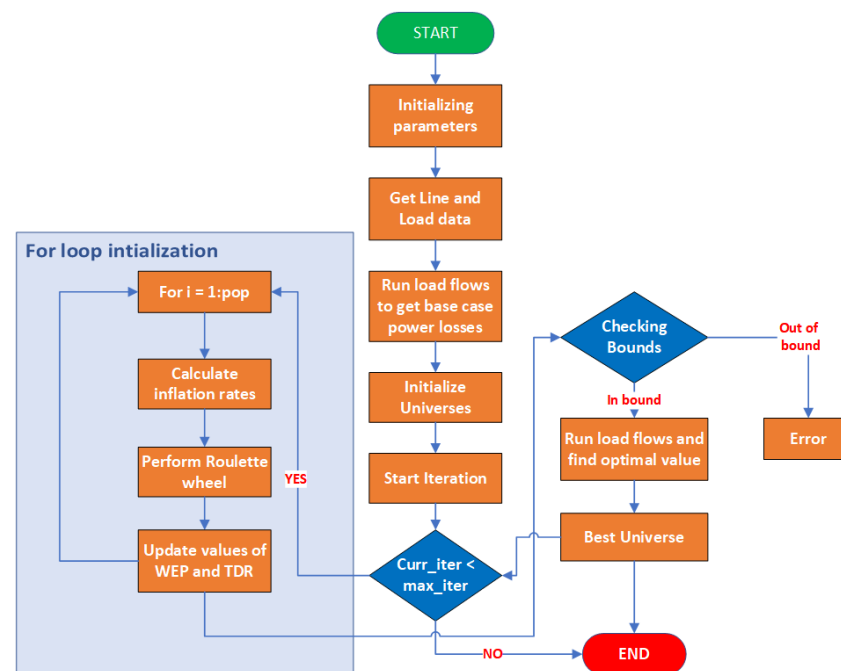


Figure 4. Flow chart of MVO.

Algorithm 2: Pseudo Code of MVO

Input: iter_max and size of population

Output: finest universe and inflation rate

Set initial parameters

Initialize universes, WEP and TDR

while curr_iter ≤ max_iter **do**

 Calculate fitness value for universes

for i = 1 : universe_size **do**

 Update WEP and TDR

for (every object) **do**

if rand1 < NSI rates (i) **then**

 White_hole_index= RWS (- NSI rates)

 Universes (BHI, j)=SU (WHL, j)

if rand2 < WEP **then**

if rand3 < 0.5 **then**

 Universes(i,j)=BU(1,j)+TDR*((ub-lb)*rand+lb)

else

 Universes (i, j) =BU(1, j)-TDR*((ub-lb)*rand+lb)

end

end

end

end

end

end

4. Results and Discussion

In this section, the validity and effectiveness of the proposed method have been tested on the IEEE 33-bus and IEEE 69-bus systems. The proposed method is simulated in a MATLAB 2020a environment on an HP PAVILION AMD RYZEN 4000 series 5, with 8

GB RAM. This research article addresses multiple objectives that include the power loss reduction, voltage deviation (VD) minimization, maximization of the voltage stability index, and energy loss cost reduction improves the energy loss cost savings and CO₂ emissions. The following cases are considered in this system to evaluate the results:

1. Without the DG (base case);
2. Three DGs at unity power factor;
3. Three DGs at 0.95 power factor;
4. Three DGs at optimal power factor.

4.1. TEE Parameters Evaluation

Table 1 shows the evaluation of the technical, economical, and environmental (TEE) indices of the IEEE 33- and 69-bus systems using the proposed ALO. The active power loss, reactive power loss, voltage deviation, and voltage stability index are considered as the technical parameters. The annual energy loss cost and the annual energy loss cost savings fall in the category of economical indices, whereas in the environmental parameters, the carbon emissions are considered.

It can be noted that the results of the technical parameters are significantly improved as compared to the base case at each power factor considered. In the optimal power factor, P_L (in kW) reduces to 11.74 from 210.9, Q_L (in kVAR) reduces to 11.2571 from 142.4355, and VSI (in p.u) increases from 0.6672 to 0.9805, which are better than the results at other p.fs, but V_D comes out to be 0.000278 p.u at 0.95 p.f which is better among other cases. Similarly in the IEEE 69-bus system, the P_L , Q_L , and VSI give better results at the OPF which are 6.38 kW, 7.0149 kVAR, and 0.9937 p.u, respectively. The voltage deviation reduces to 0.00024 p.u at 0.95 p.f which is better than 0.001291 p.u at unity and 0.000329 p.u at the optimal power factor.

Table 1. Evaluation of technical, economical, and environmental indices.

Cases	PF	Technical				Economical		Environmental
		P_L (kW)	Q_L (kVAR)	VSI (p.u)	V_D (p.u)	C_{AEL} (10 ³ PKR)	S_{AEL} (%)	C_E (10 ⁶ kg)
	Base case	210.9	142.4355	0.6672	0.13271	110.849	-	22.3540
IEEE 33	Unity	70.64	50.6117	0.8937	0.006463	37.1283	66.51	4.6286
	0.95	27.84	22.2150	0.9579	0.000278	14.6327	86.80	4.0362
	Optimal	11.74	11.2571	0.9805	0.000461	6.1705	94.43	5.6150
	Base case	224.6	101.9914	0.6832	0.09765	118.0498	-	22.9285
IEEE 69	Unity	68.68	35.1813	0.9678	0.001291	36.0982	69.42	7.1208
	0.95	21.67	14.1087	0.9885	0.00024	11.3898	90.35	6.6275
	Optimal	6.38	7.0149	0.9937	0.000329	3.3533	97.16	8.6501

C_{AEL} and S_{AEL} are considered to show the effectiveness of the proposed technique from the economical aspect, for the IEEE 33-bus system C_{AEL} (in 10³ PKR) reduces from 110.849 to 37.1283, 14.6327, and 6.1705 at unity, 0.95, and optimal p.f, respectively. By using the proposed technique, the energy loss cost savings can be increased up to 94.43% annually for the 33-bus test system. Similarly for the 69-bus test system, the C_{AEL} (in 10³ PKR) reduces from 118.0498 to 36.0982, 11.3898, and 3.3533 at unity, 0.95, and optimal p.f, respectively, and S_{AEL} can be increased up to 97.16% annually. Equations (14) and (15) can be used to calculate the carbon emissions for the base case (without DG) and other cases (with DGs), respectively. The following assumptions are made to calculate the emissions from in the base case, where we are using an oil-fired plant whose μ_e is 0.65 kg CO₂/kWh [49], and the PV is being used at unity p.f, so μ_e is taken as 0.058 kg CO₂/kWh [49]. For the other cases, the bio-mass is considered as the generation source so μ_e is taken as 0.093 kg CO₂/kWh [49].

It can be seen from Table 1 that the carbon emissions are reduced to a significant value by using the proposed method in both the 33- and 69-bus test systems. The best results for C_E (in $10^6 kg$) are 4.0362 and 6.6275 obtained at 0.95 p.f for both test systems (33 and 69), respectively.

4.2. IEEE 33-Bus System

This test system is used to test the validity of the proposed techniques. The IEEE 33-bus system has 33 buses and 32 branches. Its active and reactive power demands are 3.71 MW and 2.30 MVAR, respectively. This system has a rated voltage of 12.66 kV and a 100 MVA base. According to the power flow solution, the active and reactive power losses in the system are 210.99 kW and 143.13 kVAR, respectively. The base-case results (without the DG installation) are shown in Table 1, and Figure 5 shows a single-line diagram of the 33-bus active distribution network. The number of iterations are fixed to 150 for each case.

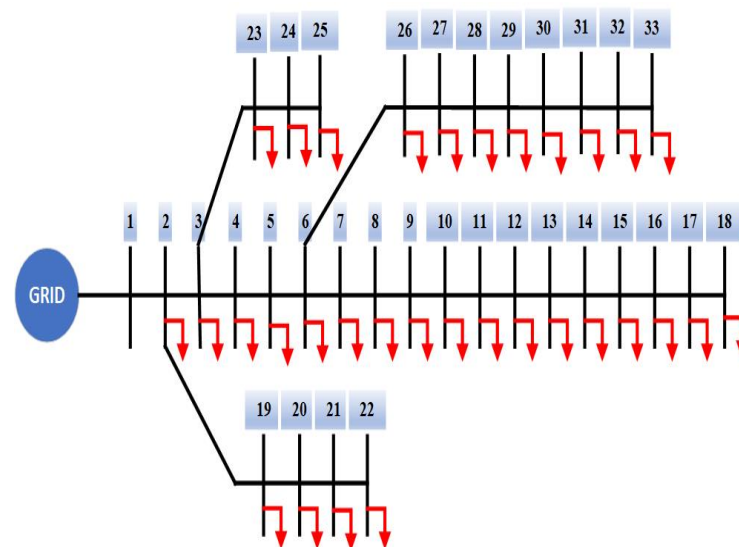


Figure 5. SLD of IEEE 33-bus system.

4.2.1. CASE 1: Three DGs at Unity P.F

The results obtained by the proposed techniques at unity power factor and their comparison with other techniques are shown in Table 2. The proposed ALO and MVO have yielded a total active power loss of 70.64 kW which is less than that of 72.785 kW from SFSA [44], 72.7869 kW from QOCSOS [53], 82.03 kW from LSFSA [54], 72.8 kW from QOSIMBO-Q [55], 75.540 kW from TLBO [56], 74.101 kW from QOTLBO [56], and 75.412 kW from KHA [57]. The annual energy loss cost (C_{AEL}) comes out to be PKR 37128.384 from the ALO and MVO which is also lower as compared to the others, such as the SFSA [44], QOCSOS [53], LSFSA [54], QOSIMBO-Q [55], TLBO [56], QOTLBO [56], and KHA [57] that optimized the cost to PKR 38255.796, PKR 38256.794, PKR 43114.968, PKR 38263.68, PKR 39703.824, PKR 38899.656, and PKR 39636.547, respectively. Similarly, the reactive power loss obtained by the ALO and MVO are 50.6117 kVAR and 50.639 3 kVAR, respectively, which are then optimized to 50.6724 kVAR from KHA [57], 50.9507 kVAR from TLBO [56], and 57.0394 kVAR from LSFSA [54]. Whereas the Q_L obtained from the proposed methods are slightly higher than that of QOTLBO [56], QOSIMO-Q [55], SFSA [44], and QOCSOS [53]. In addition to the active and reactive power loss, this paper has considered the voltage stability index (VSI) improvement and voltage deviation (V_D) reduction as objective functions to resolve the OADG problem. The VSI obtained from the MVO and ALO is 0.8939 p.u. and 0.8937 p.u., respectively, and Table 2 shows that the obtained values are better than 0.8805 p.u. from SFSA [44] and QOCSOS [53], 0.8768 p.u. from LSFSA [54], 0.8738 p.u. from SIMBO-Q [55], 0.8804 p.u. from QOSIMBO-Q [55], 0.8365 p.u. from TLBO [56], 0.8656 p.u. from QOTLBO [56], and 0.8528 p.u. from KHA [57].

Similarly, the values obtained for the V_D (in p.u.) through the proposed techniques are 0.00633 and 0.006463 which are lower than the values obtained by the QOTLBO [56], TLBO [56], QOSIMBO-Q [55], SIMBO-Q [55], QOCSOS [53], and SFSA [44] methods which are 0.0160, 0.0222, 0.0151, 0.0151, 0.0150998, and 0.015099, respectively.

Table 2. Result comparison for the IEEE 33-bus system at unity power factor.

Method	DG Size/Bus (MW)	P_L (kW) (% P_L)	Q_L (kVAR)	V_D	VSI	C_{AEL} (PKR)
SFSA [44]	0.8020/13 1.0920/24 1.0537/30	72.785 (65.50%)	49.2932	0.015099	0.8805	38255.796
QOCSOS [53]	0.8017/13 1.0913/24 1.0537/30	72.7869 (65.50%)	49.2930	0.0150998	0.8805	38256.794
LSFSA [54]	1.1124/6 0.4874/18 0.8679/30	82.03 (61.12%)	57.0394	-	0.8768	43114.968
SIMBO-Q [55]	0.7638/14 1.0415/24 1.1352/29	73.4 (65.21%)	49.9138	0.0151	0.8738	38579.04
QOSIMBO-Q [55]	0.7708/14 1.0965/24 1.0655/30	72.8 (65.50%)	49.2900	0.0151	0.8804	38263.68
TLBO [56]	0.8246/10 1.0311/24 0.8862/31	75.540 (64.20%)	50.9507	0.0222	0.8365	39703.824
QOTLBO [56]	0.8808/12 1.0592/24 1.0714/29	74.101 (64.88%)	50.3906	0.0160	0.8656	38899.656
KHA [57]	0.8107/13 0.8368/25 0.8410/30	75.412 (64.26%)	50.6724	-	0.8528	39636.547
MVO	0.875/14 1.170/24 1.212/30	70.64 (66.50%)	50.6393	0.00633	0.8939	37128.384
ALO	0.864/14 1.183/24 1.217/30	70.64 (66.50%)	50.6117	0.006463	0.8937	37128.384

4.2.2. CASE 2: Three DGs at 0.95 P.F

The optimal location and sizes of the DGs at 0.95 p.f are shown in Table 3. The MVO has placed three DGs at the 14th, 24th, and 30th bus, whereas the ALO gives the 13th, 24th, and 30th bus as the optimal locations to place the DGs. The active and reactive power losses by using the MVO are 27.84 kW and 22.4833 kVAR, respectively, and from the ant lion optimization, the P_L and Q_L come out to be 27.84 kW and 22.2150 kVAR, respectively. It may be noted from Table 3 that the proposed techniques provide better results in terms of the power loss reduction as compared to 28.5 kW from QOSIMBO-Q [55], 29 kW from SIMBO-Q [55], and 28.53 kW from SFSA [44], QOCSOS [53], and SOS [53]. The annual energy loss cost is also a minimum while using the proposed techniques as compared to the others shown in Table 3. The proposed techniques reduce the loss cost to PKR 14632.704, whereas QOSIMBO-Q [55] reduces it to PKR 14979.6, SIMBO-Q [55] to PKR 15242.4, SFSA [44] to PKR 14995.368, and QOCSOS [53] to PKR 14997.470.

The voltage deviation (in p.u.) and voltage stability index (in p.u.) are 0.000278 and 0.9579 from the proposed ALO, 0.0021 and 0.9530 from QOSIMBO-Q [55], 0.00098 and 0.9646 from SIMBO-Q [55], 0.002073 and 0.95298 from SFSA [44], and 0.002078 and 0.9530 from QOCSOS [53], respectively. The V_D and VSI obtained by the proposed technique are optimized than all the other techniques in Table 3, except SIMBO-Q [55] which gives slightly better results.

Table 3. Result comparison for the IEEE 33-bus system at 0.95 power factor.

Method	DG Size/Bus (MW)	P_L (kW) (% P_L)	Q_L (kVAR)	V_D	VSI	C_{AEL} (PKR)
QOSIMBO-Q [55]	0.8740/13	28.5 (86.49%)	20.7560	0.0021	0.9530	14979.6
	1.1830/24					
	1.3050/30					
SIMBO-Q [55]	0.9340/13	29 (86.26%)	21.0457	0.00098	0.9646	15242.4
	1.1424/24					
	1.3781/30					
SFSA [44]	0.8740/13	28.53 (86.48%)	20.7580	0.002073	0.95298	14995.368
	1.1849/24					
	1.3048/30					
QOCSOS [53]	0.8738/13	28.534 (86.48%)	20.7567	0.002078	0.9530	14997.470
	1.1838/24					
	1.3048/30					
SOS [53]	0.8738/13	28.534 (86.48%)	20.7567	0.002078	0.9530	14997.470
	1.1838/24					
	1.3048/30					
MVO	0.9340/14 1.2896/24 1.4831/30	27.84 (86.80%)	22.4833	0.000329	0.9577	14632.704
ALO	0.9673/13 1.3050/24 1.4546/30	27.84 (86.80%)	22.2150	0.000278	0.9579	14632.704

4.2.3. Case 3: Three DGs at Optimal P.F

Respecting the base case, the DGs operating at an optimal power factor reduce the active power loss by almost 94.4%, which is better than the results obtained by using other techniques, such as the SFSA [44], QOCSOS [53], and ICA/GA [58] that reduce the power losses by 94.42%, 94.43%, and 94.35%, respectively, as shown in Table 4. Similarly, using the proposed techniques at the OPF shows a significant improvement in the voltage deviation and voltage stability index results. The V_D (in p.u.) from the ALO and MVO is 0.000461 and 0.000519, respectively, whereas the VSI (in p.u.) comes out to be 0.9805 from the ALO and 0.9797 from the MVO. The V_D is 0.000619 from SFSA [44], 0.000633 from QOCSOS [53], and 0.0006 from ICA/GA [58], and similarly the VSI from SFSA [44] is 0.9691, 0.9688 from QOCSOS [53], and 0.9690 from ICA/GA [58]. The annual energy loss cost is reduced to PKR 6170.54 by the ALO, PKR 6175.8 by the MVO, PKR 6254.64 by the ICA/GA [58], and PKR 6182.107 by the SFSA [44].

Figure 6 shows the convergence curves of the proposed techniques at the unity power factor. The proposed ALO can produce a quick and steady convergence which makes it better than the MVO which shows a relatively slow convergence and takes more numbers of iterations to reach the optimal point. Figure 7 depicts the effect of the DG installation on the voltage profile of the distribution system with a different p.f. and the graph shows that integrating multiple DGs with an optimal p.f. results in a significant voltage improvement.

To decide the best case among the three cases discussed above (the unity p.f, fixed p.f, and optimal p.f), multi-criteria decision-making (MCDM) techniques such as the WSM,

WPM, TOPSIS, and VIKOR are used. Figure 8 shows that on the basis of the evaluations by each MCDM technique, case 3 (DGs operating at optimal power factors) stands out from the other cases. The active power loss at each bus for all of the cases can be seen in Figure 9, and it is clear that P_L reduces at every power factor considered with reference to the base case, but the most reduction can be noted in case 3.

Table 4. Result comparison for the IEEE 33-bus system at optimal power factor.

Method	DG Size/pf (MVA)	Location	P_L (kW) (% P_L)	Q_L (kVAR)	V_D	VSI	C_{AEL} (PKR)
SFSA [44]	0.8768/0.904	13	11.762 (94.42%)	9.9842	0.000619	0.9691	6182.107
	1.1553/0.892	24					
	1.4549/0.716	30					
QOCSOS [53]	0.8773/0.905	13	11.741 (94.43%)	9.7548	0.000633	0.9688	6171.069
	1.1884/0.900	24					
	1.4434/0.713	30					
ICA/GA [58]	0.8794/0.90	13	11.9 (94.35%)	9.7611	0.0006	0.9690	6254.64
	1.1879/0.90	24					
	1.4496/0.71	30					
MVO	0.9868/0.88	13	11.75 (94.42%)	11.4238	0.000519	0.9797	6175.8
	1.3175/0.91	24					
	1.6093/0.71	30					
ALO	0.9735/0.90	13	11.74 (94.43%)	11.2571	0.000461	0.9805	6170.544
	1.3232/0.90	24					
	1.5932/0.71	30					

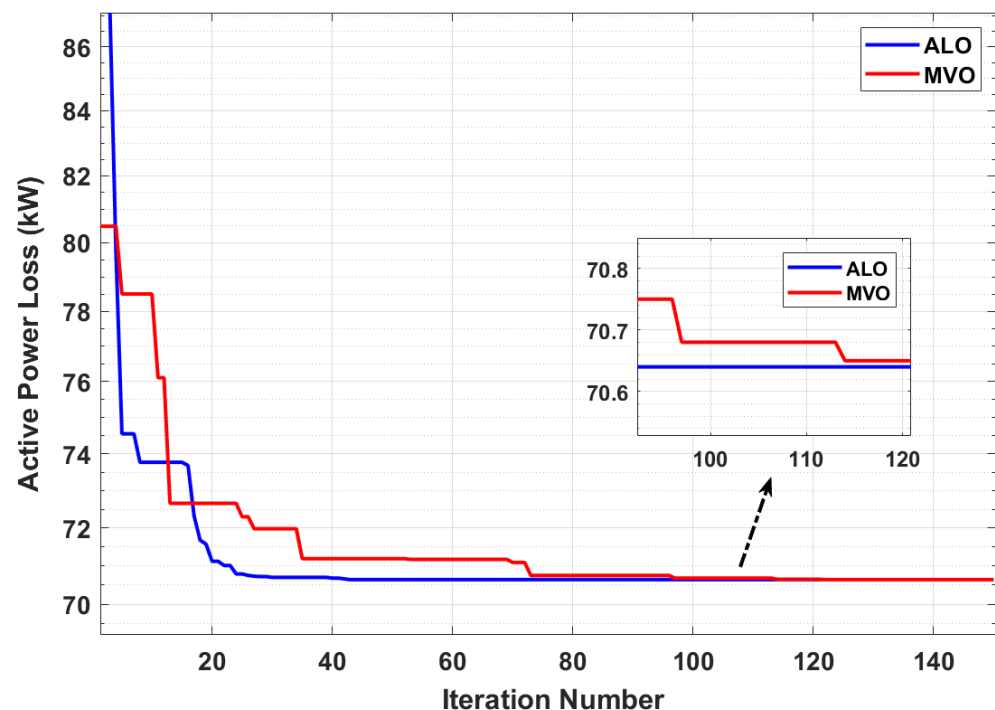


Figure 6. Convergence curve of ALO and MVO at unity p.f for IEEE 33-bus system.

Table 5 illustrates the statistical analysis across ten runs to demonstrate the efficacy of the proposed ant lion optimization (ALO) and multiverse optimization (MVO) based on the best, average, and worst values for the power losses, and the best value obtained by the proposed ALO is 70.64, 27.84, and 11.74 at the unity, 0.95, and optimal power factor, respectively. The average values obtained by the ALO are 70.70, 29.60, and 16.84 at the respective p.f.

which are better than the MVO which gives 72.87, 30.25, and 16.21, respectively. Figure 10 shows the graphical aspect of the statistical analysis discussed in Table 5, and it can be clearly seen that the ALO performs statistically better as compared to the MVO.

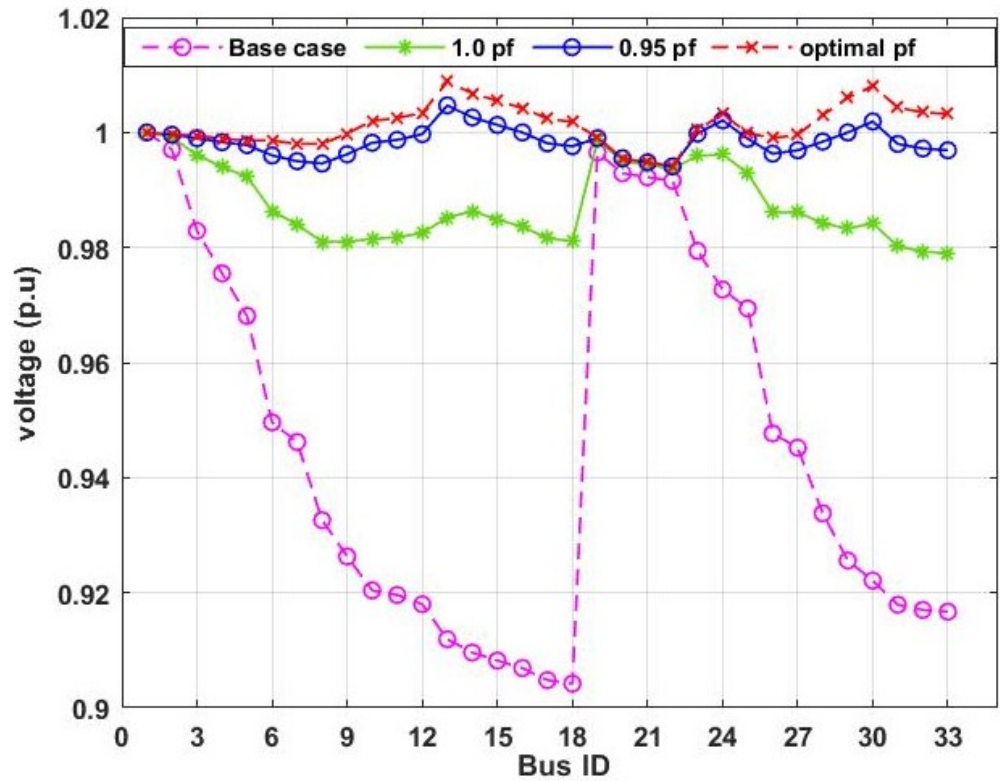


Figure 7. Voltage profile at various p.f for 33-bus system.

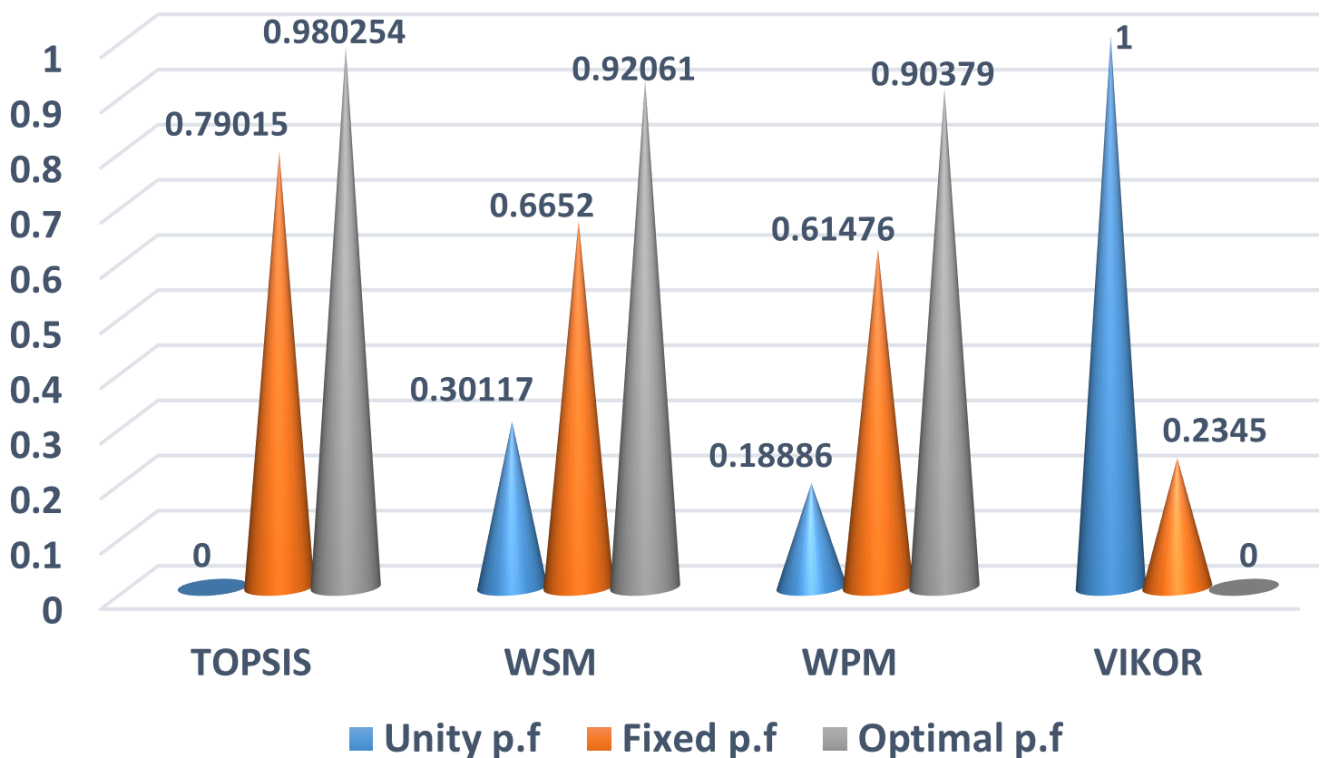


Figure 8. Cases evaluation for IEEE 33-bus system using various MCDM techniques.

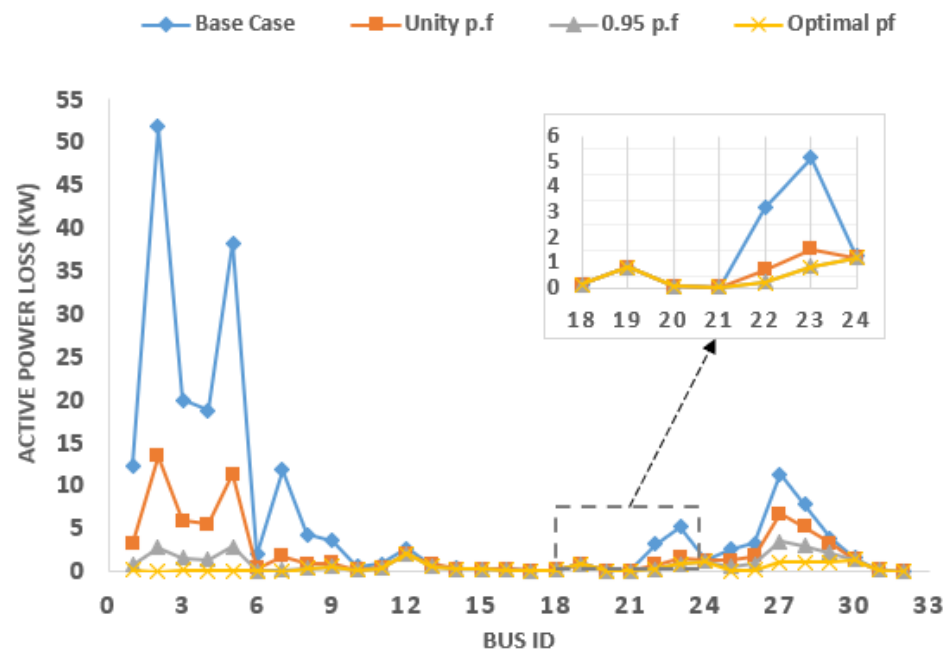


Figure 9. Active power loss at each bus considering various p.fs for IEEE 33-bus system.

Table 5. Statistical analysis for ALO and MVO for IEEE 33-bus system.

Cases		C_{Best}	$C_{Average}$	C_{Worst}
Unity p.f	ALO	70.64	70.70	71.17
	MVO	70.64	72.87	76.21
0.95 p.f	ALO	27.84	29.60	35.74
	MVO	27.84	30.25	36.68
Optimal p.f	ALO	11.74	16.84	23.80
	MVO	11.75	16.21	25.14

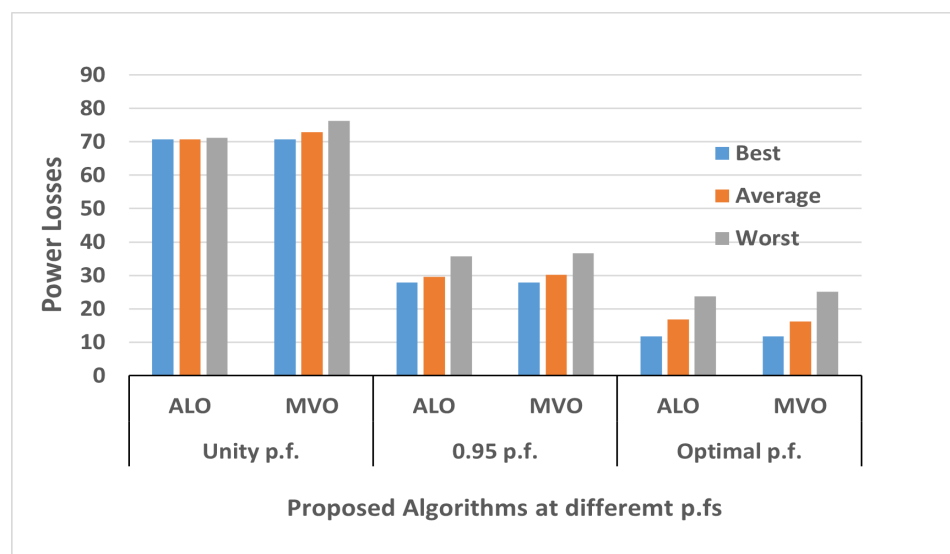


Figure 10. Graphical representation of statistical analysis for IEEE 33-bus system.

4.3. IEEE 69-Bus System

The second test system used to test the validity of the proposed techniques is the IEEE 69-bus system that has 69 buses and 68 branches. Its active and reactive power demands

are 3.80 MW and 2.69 MVAR, respectively. The number of DGs are assumed to be three, and the maximum iteration is 150 for each case. The base-case results (without the DG installation) are shown in Table 1, whereas Figure 11 shows a single-line diagram of the 69-bus test system.

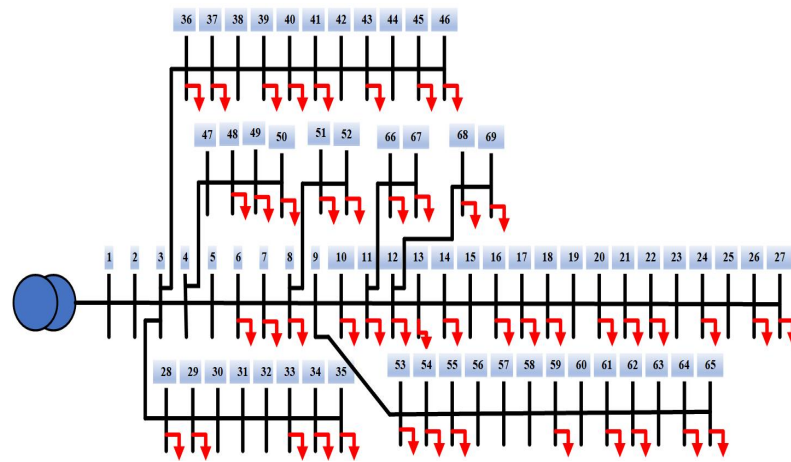


Figure 11. SLD of IEEE 69-bus system.

4.3.1. Case 1: Three DGs at Unity P.F

A multi-objective function is examined for the simultaneous minimization of the real power loss, enhancement of the voltage profile, and voltage stability index to highlight the efficacy of the presented methodologies. The findings of the ALO and MVO simulations at the unity power factor are compared to the other approaches in Table 6. The real power reduction achieved by the ALO (68.68 kW) and MVO (68.88 kW) is optimized as compared to the SFSA [44] (69.428 kW), QOCSOS [53] (69.428 kW), KHA [57] (69.563 kW), QOSIMBO-Q [55] (71 kW), MINLP [1] (69.67 kW), and QOTLBO [56] (71.625 kW). Similarly, in terms of the proposed voltage deviation and voltage stability index techniques, the ALO (0.001291 p.u. and 0.9678 p.u.) and MVO (0.001277 p.u. and 0.9676 p.u.) provide better results than the SFSA [44] (0.005185 p.u. and 0.9186 p.u.), QOCSOS [53] (0.005195 p.u. and 0.9186 p.u.), QOSIMBO-Q [55] (0.0071 p.u. and 0.8984 p.u.), and QOTLBO [56] (0.0062 p.u. and 0.9196 p.u.). The annual energy loss cost is reduced to PKR 36098.208 which is better than PKR 36491.359 by SFSA [44], PKR 36491.356 by QOCSOS [53], PKR 36562.312 by KHA [57], and PKR 36618.552 by MINLP [1].

Table 6. Result comparison for the IEEE 69-bus system at unity power factor.

Method	DG Size/Bus (MW)	P_L (kW) (% P_L)	Q_L (kVAR)	V_D	VSI	C_{AEL} (PKR)
SFSA [44]	0.5273/11	69.428	34.6278	0.005185	0.9186	36491.356
	0.3805/18	(69.14%)				
	1.7198/61					
QOCSOS [53]	0.5269/11	69.428	34.6283	0.005195	0.9186	36491.356
	0.3803/18	(69.14%)				
	1.7190/61					
KHA [57]	0.4962/12	69.563	34.6515	-	0.9185	36562.312
	0.3113/22	(69.08%)				
	1.7354/61					
QOSIMBO-Q [55]	0.8336/9	71	35.4736	0.0071	0.8984	37317.6
	0.4511/18	(68.44%)				
	1.5000/61					

Table 6. Cont.

Method	DG Size/Bus (MW)	P_L (kW) (% P_L)	Q_L (kVAR)	V_D	VSI	C_{AEL} (PKR)
MINLP [1]	1.7200/61	69.67	34.6286	-	-	36618.552
	0.3800/17	(69.07%)				
	0.5300/11					
QOTLBO [56]	0.5334/18	71.625	35.3462	0.0062	0.9196	37646.1
	1.1986/61	(68.17%)				
	0.5672/63					
MVO	1.9400/61	68.88	35.2731	0.001277	0.9676	36302.328
	0.4610/66	(69.33%)				
	0.447/17					
ALO	1.925/61	68.68	35.1813	0.001291	0.9678	36098.208
	0.427/17	(66.50%)				
	0.525/11					

4.3.2. Case 2: Three DGs at 0.95 P.F

Table 7 presents a comparison of the findings of the IEEE 69-bus test system at 0.95 p.f. It can be seen that the power losses are reduced to 90.33% and 90.35% by using the proposed MVO and ALO, respectively, which are better than 89.87% from QOSIMBO-Q [55] and 89.73% from SIMBO-Q [55]. Similarly, the V_D (in p.u.) and VSI (in p.u.) obtained by the MVO (0.00019 and 0.9870) and ALO (0.00024 and 0.9885) are better than the QOSIMBO-Q [55] (0.00069 and 0.9741) and SIMBO-Q [55] (0.00075 and 0.9727). It may be noted from Table 7 that the proposed techniques provide preferable results in terms of the reactive power loss (Q_L) and annual energy loss cost (C_{AEL}) as compared to other techniques. The Q_L is reduced to 14.1087kVAR by ALO, 11405.52kVAR by MVO, 12141.36kVAR by SIMBO-Q [55], and 11983.68kVAR by QOSIMBO-Q [55].

Table 7. Result comparison for the IEEE 69-bus system at 0.95 power factor.

Method	DG Size/Bus (MW)	P_L (kW) (% P_L)	Q_L (kVAR)	V_D	VSI	C_{AEL} (PKR)
QOSIMBO-Q [55]	0.4497/64	22.8	14.6602	0.00069	0.9741	11983.68
	0.6135/17	(89.87%)				
	1.5789/61					
SIMBO-Q [55]	0.5954/19	23.1	14.7630	0.00075	0.9727	12141.36
	1.5789/61	(89.73%)				
	0.4442/64					
MVO	2.000/61	21.70	13.9685	0.00019	0.9870	11405.52
	0.6674/11	(90.33%)				
	0.4947/19					
ALO	0.8358/11	21.67	14.1087	0.00024	0.9885	11389.752
	0.4316/21	(90.35%)				
	2.000/61					

4.3.3. Case 3: Three DGs at Optimal P.F

In this scenario, the real power losses are reduced to 97.16% and 97.15% as compared to the base case, whereas the Q_L is reduced to 6.9941 kVAR and 7.0149 kVAR by using the MVO and ALO, respectively. Table 8 shows a comparison of the real and reactive power loss reduction with other techniques from the literature, such as the HHO [2] and SFSA [44], and the efficacy of the proposed techniques is very clear. The voltage deviation (in p.u.) and voltage stability index (in p.u.) are also improved by using the proposed ALO (0.000329 and 0.9937) and MVO (0.000319 and 0.9929). Table 8 shows a comparison of the results from

the proposed methods with the HHO [2] and SFSA [44]. In comparison to the HHO [2], which reduces the active power loss to 6.58 kW, the reactive power loss to 7.5492 kVAR, and the yearly energy loss cost to 3458.448 PKR, the proposed solutions give a better loss reduction and cost reduction. Alternatively, the SFSA [44] has a better P_L reduction of 4.298 kW and Q_L a reduction of 6.7597 kVAR as compared to the suggested techniques, but the VSI is 0.9773 p.u which is lower than the ALO (0.9937 p.u) and MVO (0.9929 p.u).

Figure 12 shows the convergence curve of the proposed techniques at unity power factors for IEEE 69-bus system. The proposed ALO can produce a quick and steady convergence. The multi-criteria decision-making (MCDM) techniques such as the WSM, WPM, TOPSIS, and VIKOR are used to choose the best case among the different power factors (the unity p.f, fixed p.f, and optimal p.f) by treating all the objectives equally and assigning equal weights to them. Figure 13 depicts the effect of the DG installation on the voltage profile of the distribution system with a different p.f. and the graph shows that integrating multiple DGs with the optimal p.f. results in a significant voltage improvement.

Figure 14 illustrates that, based on the evaluations by each MCDM technique, case 3 (DGs operating at optimal power factor) stands out from the others. The active power loss at each bus for all of the cases can be seen in Figure 15, and it is clear that P_L reduces at every power factor considered with reference to the base case, but the most reduction can be noted in case 3. Table 9 illustrates the statistical analysis across ten runs to demonstrate the efficacy of the proposed ant lion optimization (ALO) and multiverse optimization (MVO) based on the best, average, and worst values for the power losses. The best value obtained by the proposed ALO is 68.68, 21.67, and 6.38 at the unity, 0.95, and optimal power factor, respectively. The average values obtained by the ALO are 70.17, 24.62, and 11.02 at the respective p.f. which are better than the MVO which gives 71.06, 24.88, and 11.93, respectively. Figure 16 shows the graphical aspect of the statistical analysis discussed in Table 9, and it can be clearly seen that the ALO performs statistically better as compared to the MVO.

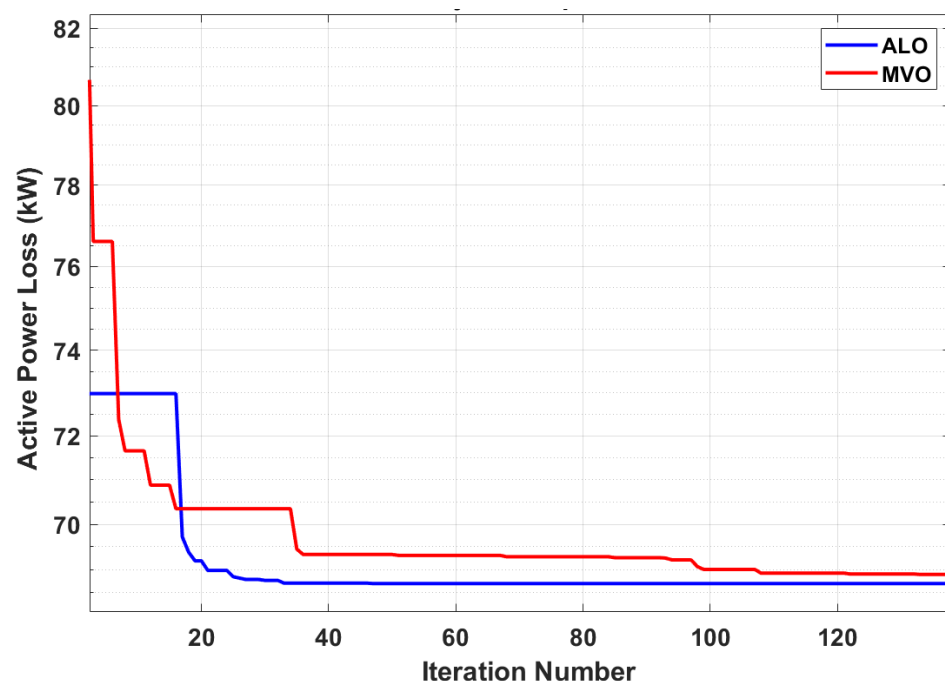


Figure 12. Convergence curve of ALO and MVO at unity p.f for IEEE 69-bus system.

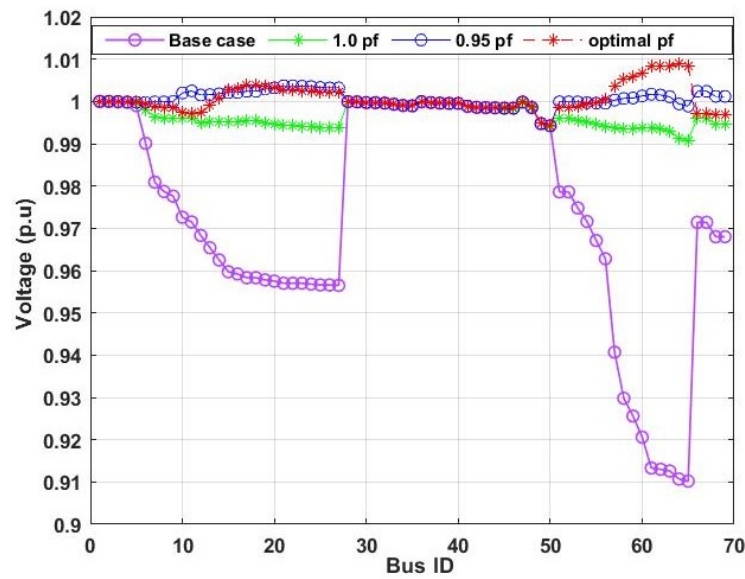


Figure 13. Voltage profile at various p.f for 69-bus system.

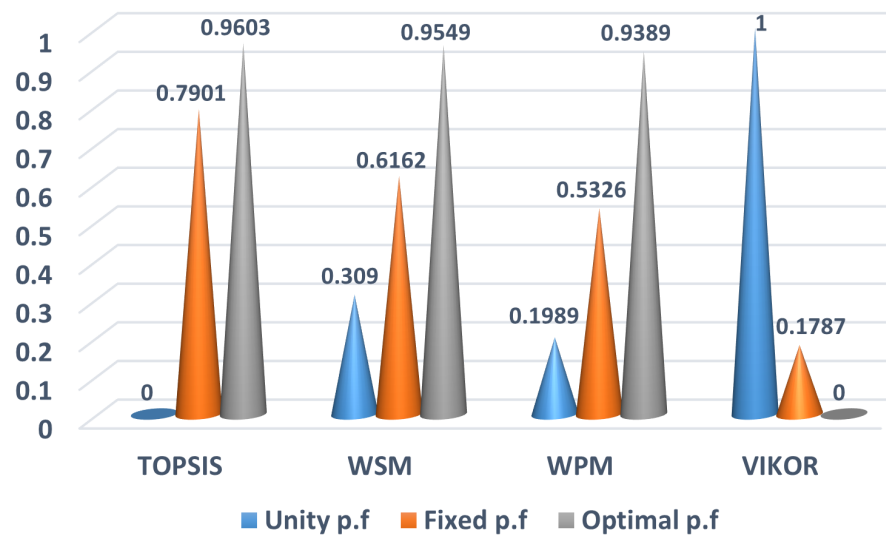


Figure 14. Cases evaluation for IEEE 69-bus system using various MCDM techniques.

Table 8. Result comparison for the IEEE 69-bus system at optimal power factor.

Method	DG Size/pf (MVA)	Location	P_L (kW) (% P_L)	Q_L (kVAR)	V_D	VSI	C_{AEL} (PKR)
HHO [2]	0.4711/0.57	17	6.58 (97.07%)	7.5492	-	-	3458.448
	2.0169/0.76	61					
	0.7191/0.97	66					
SFSA [44]	0.4711/0.819	11	4.298 (98.09%)	6.7597	0.000116	0.9773	2259.028
	2.0169/0.833	21					
	0.7191/0.818	61					
MVO	0.5231/0.82	17	6.36 (97.16%)	6.9941	0.000319	0.9929	3342.816
	0.8275/0.80	11					
	2.0123/0.81	61					
ALO	0.4672/0.82	21	6.38 (97.15%)	7.0149	0.000329	0.9937	3353.328
	1.9998/0.80	61					
	0.8609/0.80	11					

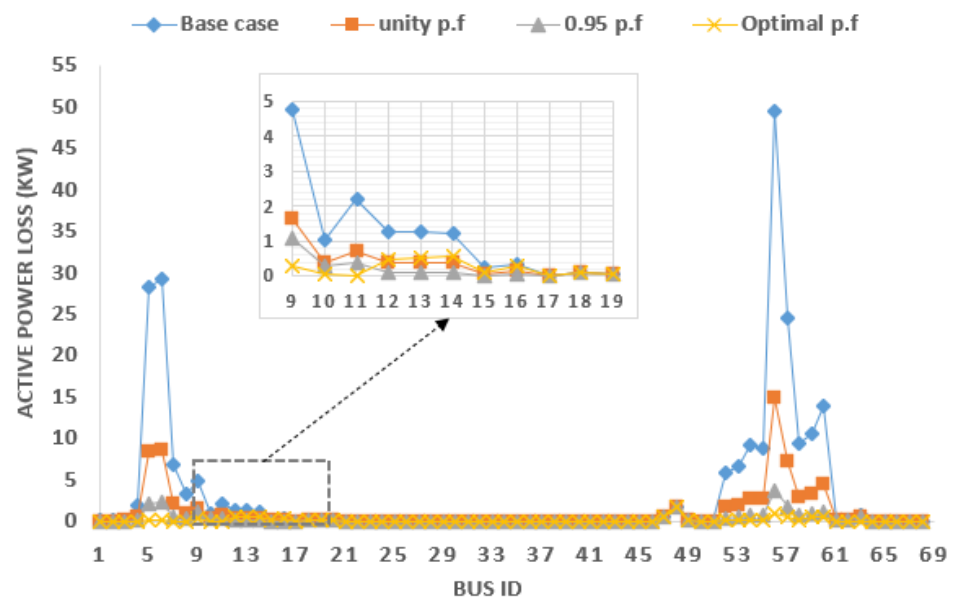


Figure 15. Active power loss at each bus considering various p.fs for IEEE 33-bus system.

Table 9. Statistical analysis for ALO and MVO for IEEE 69-bus system.

Cases		C_{Best}	$C_{Average}$	C_{Worst}
Unity p.f	ALO	68.68	70.17	73.04
	MVO	68.88	71.06	73.36
0.95 p.f	ALO	21.67	24.62	28.44
	MVO	21.70	24.88	27.61
Optimal p.f	ALO	6.38	11.02	16.02
	MVO	6.36	11.93	18.11

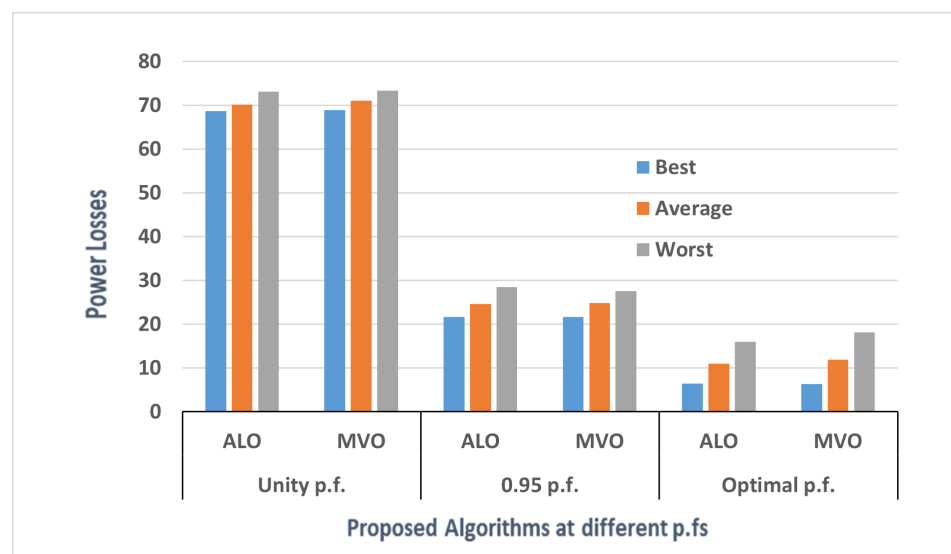


Figure 16. Graphical representation of statistical analysis for IEEE 69-bus system.

5. Conclusions

In this study, the proposed ALO and MVO were adopted to reduce the power loss, voltage profile, VSI, energy loss cost, and carbon emissions in ADNs. The MCDM techniques such as the WSM, WPM, TOPSIS, and VIKOR were used to solve the multi-objective issue

and choose the optimum scenario. The suggested ALO was compared to the MVO based on a statistical analysis and a convergence curve. The results showed that the ALO has a better and faster convergence than the MVO and is superior in attaining the optimal DG allocation in the ADN. The techniques suggested have been tested on standard IEEE 33- and 69-bus systems at different p.f. levels of operation. The results obtained by the proposed algorithm revealed that the highest loss reduction in the IEEE 33- and 69-bus systems was 94.43% and 97.16%, respectively, and the maximum VSI was 0.9805 p.u and 0.9937 p.u, respectively; moreover, the minimum V_D for the given test systems was 0.00019 p.u. For both test systems, C_{AEL} gives the highest reduction in case 3 as 6170.5 PKR and 3353.3 PKR from 110849 PKR and 118049.8 PKR, respectively, whereas the carbon emissions also show a significant reduction. Among the many DG operation modes, the scenario of the DGs operating at the optimal power factor has been shown to significantly improve the results.

Future research should investigate the proper distribution of DGs from the perspective of varying levels of DG penetration at dynamic loading. In addition, the effects of the intermittent nature of a renewable DG could be mitigated by the use of uncertainty modeling.

Author Contributions: Conceptualization, S.A.A.K., A.A. and Z.A.K.; methodology, S.A.A.K., Z.A.K. and A.A.; software, M.S.S.; validation, M.S.S., S.A.A.K. and Z.A.K.; formal analysis, M.S.S. and A.A.; investigation, M.S.S.; resources, Z.A.K. and A.A.; data curation, M.S.S. and A.A.; writing—original draft preparation, M.S.S. and S.A.A.K.; writing—review and editing, Z.A.K., A.A. and D.R.S.; visualization, M.S.S.; supervision, S.A.A.K. and Z.A.K.; project administration, S.A.A.K., Z.A.K. and A.A.; funding acquisition, A.A. All authors have read and agreed to the published version of the manuscript.

Funding: This work is funded by the Deanship of Scientific Research at Majmaah University under Project Number No. R-2023-34.

Institutional Review Board Statement: Not applicable.

Informed Consent Statement: Not applicable.

Data Availability Statement: Not applicable.

Acknowledgments: The author would like to thank the Deanship of Scientific Research at Majmaah University for supporting this work under Project Number No. R-2023-34.

Conflicts of Interest: The authors declare no conflict of interest.

Abbreviations

The following abbreviations were used in this paper.

DG	Distributed generation
p.f	Power factor
ADN	Active distribution network
MCDM	Multi-criteria decision making
OADG	Optimal allocation of distributed generation
P_L	Active power loss
Q_L	Reactive power loss
V_D	Voltage deviation
VSI	Voltage stability index
C_E	Carbon emissions
GHG	Greenhouse gas
C_{AEL}	Annual energy loss cost
S_{AEL}	Annual energy loss cost savings
p.u	Per unit
PLC	Power loss cost
PLS	Power loss savings
WSM	Weighted sum method
MILP	Mixed-integer linear programming
WPM	Weighted product method
ALO	Ant lion optimization

MVO	Multiverse optimization
SOOP	Single-objective optimization problem
MOOP	Multi objective optimization problem
V_{ref}	Reference voltage (1.0 p.u)
μ_e	Emissions rate
I_b	Branch current
X_b	Branch reactance
P_{Gen}	Active power generation
Q_{Gen}	Reactive power generation
LSF	Load sensitivity factor
DERs	Distributed energy resources
G_E	Energy generated by grid
DG_E	Energy generated by DG
μ_E	Rate of energy (\$/kWh)
Iter_max	Maximum number of iterations
rand	Random number
norinf	Normal inflation
curr_iter	Current iteration
OPF	Optimal power factor
UPF	Unity power factor

References

1. Kaur, S.; Kumbhar, G.; Sharma, J. A MINLP technique for optimal placement of multiple DG units in distribution systems. *Int. J. Electr. Power Energy Syst.* **2014**, *63*, 609–617. [\[CrossRef\]](#)
2. Selim, A.; Kamel, S.; Alghamdi, A.S.; Jurado, F. Optimal placement of DGs in distribution system using an improved harris hawks optimizer based on single-and multi-objective approaches. *IEEE Access* **2020**, *8*, 52815–52829. [\[CrossRef\]](#)
3. Ali, A.; Raisz, D.; Mahmoud, K. Optimal oversizing of utility-owned renewable DG inverter for voltage rise prevention in MV distribution systems. *Int. J. Electr. Power Energy Syst.* **2019**, *105*, 500–513. [\[CrossRef\]](#)
4. Mirjalili, S. The ant lion optimizer. *Adv. Eng. Softw.* **2015**, *83*, 80–98. [\[CrossRef\]](#)
5. Mirjalili, S.; Mirjalili, S.M.; Hatamlou, A. Multi-verse optimizer: A nature-inspired algorithm for global optimization. *Neural Comput. Appl.* **2016**, *27*, 495–513. [\[CrossRef\]](#)
6. Chopra, N.; Mehta, S. Multi-objective optimum generation scheduling using Ant Lion Optimization. In Proceedings of the 2015 Annual IEEE India Conference (INDICON), New Delhi, India, 17–20 December 2015; IEEE: Piscataway, NJ, USA, 2015; pp. 1–6.
7. Petrović, M.; Petronijević, J.; Mitić, M.; Vuković, N.; Plemić, A.; Miljković, Z.; Babić, B. The ant lion optimization algorithm for flexible process planning. *J. Prod. Eng.* **2015**, *18*, 65–68.
8. Talatahari, S. Optimum design of skeletal structures using ant lion optimizer. *Iran Univ. Sci. Technol.* **2016**, *6*, 13–25.
9. Ehsan, A.; Yang, Q. Optimal integration and planning of renewable distributed generation in the power distribution networks: A review of analytical techniques. *Appl. Energy* **2018**, *210*, 44–59. [\[CrossRef\]](#)
10. Hung, D.Q.; Mithulananthan, N.; Bansal, R. Analytical expressions for DG allocation in primary distribution networks. *IEEE Trans. Energy Convers.* **2010**, *25*, 814–820. [\[CrossRef\]](#)
11. Gözel, T.; Hocaoglu, M.H. An analytical method for the sizing and siting of distributed generators in radial systems. *Electr. Power Syst. Res.* **2009**, *79*, 912–918. [\[CrossRef\]](#)
12. Hung, D.Q.; Mithulananthan, N. Multiple distributed generator placement in primary distribution networks for loss reduction. *IEEE Trans. Ind. Electron.* **2011**, *60*, 1700–1708. [\[CrossRef\]](#)
13. Lee, S.H.; Park, J.W. Selection of optimal location and size of multiple distributed generations by using Kalman filter algorithm. *IEEE Trans. Power Syst.* **2009**, *24*, 1393–1400.
14. Ochoa, L.F.; Harrison, G.P. Minimizing energy losses: Optimal accommodation and smart operation of renewable distributed generation. *IEEE Trans. Power Syst.* **2010**, *26*, 198–205. [\[CrossRef\]](#)
15. Rueda-Medina, A.C.; Franco, J.F.; Rider, M.J.; Padilha-Feltrin, A.; Romero, R. A mixed-integer linear programming approach for optimal type, size and allocation of distributed generation in radial distribution systems. *Electr. Power Syst. Res.* **2013**, *97*, 133–143. [\[CrossRef\]](#)
16. Abu-Mouti, F.S.; El-Hawary, M. Optimal distributed generation allocation and sizing in distribution systems via artificial bee colony algorithm. *IEEE Trans. Power Deliv.* **2011**, *26*, 2090–2101. [\[CrossRef\]](#)
17. Shukla, T.; Singh, S.; Srinivasarao, V.; Naik, K. Optimal sizing of distributed generation placed on radial distribution systems. *Electr. Power Components Syst.* **2010**, *38*, 260–274. [\[CrossRef\]](#)
18. Gomez-Gonzalez, M.; López, A.; Jurado, F. Optimization of distributed generation systems using a new discrete PSO and OPF. *Electr. Power Syst. Res.* **2012**, *84*, 174–180. [\[CrossRef\]](#)
19. Kansal, S.; Kumar, V.; Tyagi, B. Hybrid approach for optimal placement of multiple DGs of multiple types in distribution networks. *Int. J. Electr. Power Energy Syst.* **2016**, *75*, 226–235. [\[CrossRef\]](#)

20. Wang, C.; Nehrir, M.H. Analytical approaches for optimal placement of distributed generation sources in power systems. *IEEE Trans. Power Syst.* **2004**, *19*, 2068–2076. [[CrossRef](#)]
21. Borghetti, A. A mixed-integer linear programming approach for the computation of the minimum-losses radial configuration of electrical distribution networks. *IEEE Trans. Power Syst.* **2012**, *27*, 1264–1273. [[CrossRef](#)]
22. Selim, A.; Kamel, S.; Mohamed, A.A.; Elattar, E.E. Optimal Allocation of Multiple Types of Distributed Generations in Radial Distribution Systems Using a Hybrid Technique. *Sustainability* **2021**, *13*, 6644. [[CrossRef](#)]
23. Soroudi, A.; Afrasiab, M. Binary PSO-based dynamic multi-objective model for distributed generation planning under uncertainty. *IET Renew. Power Gener.* **2012**, *6*, 67–78. [[CrossRef](#)]
24. Kumar, S.; Mandal, K.K.; Chakraborty, N. Optimal placement of different types of DG units considering various load models using novel multiobjective quasi-oppositional grey wolf optimizer. *Soft Comput.* **2021**, *25*, 4845–4864. [[CrossRef](#)]
25. Khalesi, N.; Rezaei, N.; Haghifam, M.R. DG allocation with application of dynamic programming for loss reduction and reliability improvement. *Int. J. Electr. Power Energy Syst.* **2011**, *33*, 288–295. [[CrossRef](#)]
26. Moradi, M.H.; Abedini, M. A combination of genetic algorithm and particle swarm optimization for optimal DG location and sizing in distribution systems. *Int. J. Electr. Power Energy Syst.* **2012**, *34*, 66–74. [[CrossRef](#)]
27. Moradi, M.; Abedini, M. A novel method for optimal DG units capacity and location in Microgrids. *Int. J. Electr. Power Energy Syst.* **2016**, *75*, 236–244. [[CrossRef](#)]
28. Mohamed Imran, A.; Kowsalya, M. Optimal size and siting of multiple distributed generators in distribution system using bacterial foraging optimization. *Swarm Evol. Comput.* **2014**, *15*, 58–65. [[CrossRef](#)]
29. Kefayat, M.; Ara, A.L.; Niaki, S.N. A hybrid of ant colony optimization and artificial bee colony algorithm for probabilistic optimal placement and sizing of distributed energy resources. *Energy Convers. Manag.* **2015**, *92*, 149–161. [[CrossRef](#)]
30. Harrison, G.P.; Piccolo, A.; Siano, P.; Wallace, A.R. Hybrid GA and OPF evaluation of network capacity for distributed generation connections. *Electr. Power Syst. Res.* **2008**, *78*, 392–398. [[CrossRef](#)]
31. Khatod, D.K.; Pant, V.; Sharma, J. Evolutionary programming based optimal placement of renewable distributed generators. *IEEE Trans. Power Syst.* **2012**, *28*, 683–695. [[CrossRef](#)]
32. Celli, G.; Ghiani, E.; Mocchi, S.; Pilo, F. A multiobjective evolutionary algorithm for the sizing and siting of distributed generation. *IEEE Trans. Power Syst.* **2005**, *20*, 750–757. [[CrossRef](#)]
33. Wang, L.; Singh, C. Reliability-constrained optimum placement of reclosers and distributed generators in distribution networks using an ant colony system algorithm. *IEEE Trans. Syst. Man Cybern. Part C* **2008**, *38*, 757–764. [[CrossRef](#)]
34. Ramadan, A.; Ebeed, M.; Kamel, S.; Nasrat, L. Optimal allocation of renewable energy resources considering uncertainty in load demand and generation. In Proceedings of the 2019 IEEE Conference on Power Electronics and Renewable Energy (CPERE), Aswan City, Egypt, 23–25 October 2019; IEEE: Piscataway, NJ, USA, 2019; pp. 124–128.
35. Prasad, C.H.; Subbaramaiah, K.; Sujatha, P. Cost-benefit analysis for optimal DG placement in distribution systems by using elephant herding optimization algorithm. *Renewables Wind. Water, Sol.* **2019**, *6*, 1–12. [[CrossRef](#)]
36. Remha, S.; Chettih, S.; Arif, S. A novel multi-objective bat algorithm for optimal placement and sizing of distributed generation in radial distributed systems. *Adv. Electr. Electron. Eng.* **2018**, *15*, 736–746. [[CrossRef](#)]
37. Hemeida, M.G.; Ibrahim, A.A.; Mohamed, A.A.A.; Alkhalaf, S.; El-Dine, A.M.B. Optimal allocation of distributed generators DG based Manta Ray Foraging Optimization algorithm (MRFO). *Ain Shams Eng. J.* **2021**, *12*, 609–619. [[CrossRef](#)]
38. Nagaballi, S.; Kale, V.S. Pareto optimality and game theory approach for optimal deployment of DG in radial distribution system to improve techno-economic benefits. *Appl. Soft Comput.* **2020**, *92*, 106234. [[CrossRef](#)]
39. Oda, E.S.; Abd El Hamed, A.M.; Ali, A.; Elbaset, A.A.; Abd El Sattar, M.; Ebeed, M. Stochastic optimal planning of distribution system considering integrated photovoltaic-based DG and DSTATCOM under uncertainties of loads and solar irradiance. *IEEE Access* **2021**, *9*, 26541–26555. [[CrossRef](#)]
40. Sun, C.; Mi, Z.; Ren, H.; Jing, Z.; Lu, J.; Watts, D. Multi-dimensional indexes for the sustainability evaluation of an active distribution network. *Energies* **2019**, *12*, 369. [[CrossRef](#)]
41. Kamble, S.G.; Vadirajacharya, K.; Patil, U.V. Decision Making in Power Distribution System Reconfiguration by Blended Biased and Unbiased Weightage Method. *J. Sens. Actuator Netw.* **2019**, *8*, 20. [[CrossRef](#)]
42. Paterakis, N.G.; Mazza, A.; Santos, S.F.; Erdinç, O.; Chicco, G.; Bakirtzis, A.G.; Catalão, J.P. Multi-objective reconfiguration of radial distribution systems using reliability indices. *IEEE Trans. Power Syst.* **2015**, *31*, 1048–1062. [[CrossRef](#)]
43. Tanwar, S.S.; Khatod, D. Techno-economic and environmental approach for optimal placement and sizing of renewable DGs in distribution system. *Energy* **2017**, *127*, 52–67. [[CrossRef](#)]
44. Nguyen, T.P.; Vo, D.N. A novel stochastic fractal search algorithm for optimal allocation of distributed generators in radial distribution systems. *Appl. Soft Comput.* **2018**, *70*, 773–796. [[CrossRef](#)]
45. Kayal, P.; Chanda, C. Placement of wind and solar based DGs in distribution system for power loss minimization and voltage stability improvement. *Int. J. Electr. Power Energy Syst.* **2013**, *53*, 795–809. [[CrossRef](#)]
46. Anbuchandran, S.; Rengaraj, R.; Bhuvanesh, A.; Karuppasamyandiyani, M. A multi-objective optimum distributed generation placement using firefly algorithm. *J. Electr. Eng. Technol.* **2022**, *17*, 945–953. [[CrossRef](#)]
47. Kazmi, S.A.A.; Ameer Khan, U.; Ahmad, W.; Hassan, M.; Ibupoto, F.A.; Bukhari, S.B.A.; Ali, S.; Malik, M.M.; Shin, D.R. Multiple (TEES)-Criteria-Based Sustainable Planning Approach for Mesh-Configured Distribution Mechanisms across Multiple Load Growth Horizons. *Energies* **2021**, *14*, 3128. [[CrossRef](#)]

48. Chiradeja, P.; Ramakumar, R. An approach to quantify the technical benefits of distributed generation. *IEEE Trans. Energy Convers.* **2004**, *19*, 764–773. [[CrossRef](#)]
49. Baldwin, S. Carbon footprint of electricity generation. *Lond. Parliam. Off. Sci. Technol.* **2006**, *268*, 1–4.
50. Scharf, I.; Subach, A.; Ovadia, O. Foraging behaviour and habitat selection in pit-building antlion larvae in constant light or dark conditions. *Anim. Behav.* **2008**, *76*, 2049–2057. [[CrossRef](#)]
51. Scharf, I.; Ovadia, O. Factors influencing site abandonment and site selection in a sit-and-wait predator: A review of pit-building antlion larvae. *J. Insect Behav.* **2006**, *19*, 197–218. [[CrossRef](#)]
52. Nischal, M.M.; Mehta, S. Optimal load dispatch using ant lion optimization. *Int. J. Eng. Res. Appl.* **2015**, *5*, 10–19.
53. Truong, K.H.; Nallagownden, P.; Elamvazuthi, I.; Vo, D.N. A quasi-oppositional-chaotic symbiotic organisms search algorithm for optimal allocation of DG in radial distribution networks. *Appl. Soft Comput.* **2020**, *88*, 106067. [[CrossRef](#)]
54. Injeti, S.K.; Kumar, N.P. A novel approach to identify optimal access point and capacity of multiple DGs in a small, medium and large scale radial distribution systems. *Int. J. Electr. Power Energy Syst.* **2013**, *45*, 142–151. [[CrossRef](#)]
55. Sharma, S.; Bhattacharjee, S.; Bhattacharya, A. Quasi-Oppositional Swine Influenza Model Based Optimization with Quarantine for optimal allocation of DG in radial distribution network. *Int. J. Electr. Power Energy Syst.* **2016**, *74*, 348–373. [[CrossRef](#)]
56. Sultana, S.; Roy, P.K. Multi-objective quasi-oppositional teaching learning based optimization for optimal location of distributed generator in radial distribution systems. *Int. J. Electr. Power Energy Syst.* **2014**, *63*, 534–545. [[CrossRef](#)]
57. Sultana, S.; Roy, P.K. Krill herd algorithm for optimal location of distributed generator in radial distribution system. *Appl. Soft Comput.* **2016**, *40*, 391–404. [[CrossRef](#)]
58. Moradi, M.H.; Zeinalzadeh, A.; Mohammadi, Y.; Abedini, M. An efficient hybrid method for solving the optimal sitting and sizing problem of DG and shunt capacitor banks simultaneously based on imperialist competitive algorithm and genetic algorithm. *Int. J. Electr. Power Energy Syst.* **2014**, *54*, 101–111. [[CrossRef](#)]

Disclaimer/Publisher’s Note: The statements, opinions and data contained in all publications are solely those of the individual author(s) and contributor(s) and not of MDPI and/or the editor(s). MDPI and/or the editor(s) disclaim responsibility for any injury to people or property resulting from any ideas, methods, instructions or products referred to in the content.